Hardware and Software for Hand-held Electrical Impedance Myography Measurement Prototype System

by

Roshni C. Cooper

S.B., Electrical Engineering and Computer Science
Massachusetts Institute of Technology, 2007

Submitted to the Department of Electrical Engineering and Computer Science

in Partial Fulfillment of the Requirements for the Degree of

Master of Engineering in Electrical Engineering and Computer Science

at the

MASSACHUSETTS INSTITUTE OF TECHNOLOGY

May 2008

Author .....

Department of Electrical Engineering and Computer Science
May 23, 2008

Certified by .....

Joel L. Dawson
Assistant Professor
Thesis Supervisor

Accepted by .....

Arthur C. Smith
Professor of Electrical Engineering
Chairman, Department Committee on Graduate Theses

Hardware and Software for Hand-held Electrical Impedance Myography Measurement Prototype System

by

Roshni C. Cooper

Submitted to the

Department of Electrical Engineering and Computer Science

May 23, 2008

In Partial Fulfillment of the Requirements for the Degree of

Master of Engineering in Electrical Engineering and Computer Science

Abstract

This thesis discusses the need for a more quantitative, objective, and non-invasive method of neuromuscular disease assessment. Currently, the best solution to this problem requires large, bulky pieces of equipment and the time-consuming placement of numerous individual electrodes. In this thesis, a new hardware device and its corresponding software interface are described. The device includes a reconfigurable hand-held probe with an electrode head which both makes contact with the skin and eliminates the need for individual electrodes. The new software interface provides a simple way for users to control the device through the USB interface of a laptop. In addition, various strategies were explored for leveraging the linearity of the muscle tissue in order to shorten the measurement time.

Thesis Supervisor: Joel L. Dawson
Title: Assistant Professor

Acknowledgments

I first thank my thesis advisor, Professor Joel Dawson for inviting me to join this exciting project last year. He has been a very insightful and supportive advisor, making my experience with this project thoroughly educational and enjoyable.

Special thanks to Dr. Seward Rutkove for making this project possible with his insight into the relationships between electrical engineering and neurology. His expertise in electrical impedance myography added a valuable perspective to my experience.

Additionally, I thank my fellow students working with this project, Michael Scharfstein, Muyiwa Ogunikka, and Hong Ma. They quickly brought me up to speed with the project when I joined, and they were always willing to provide me with information and advice during my research.

Finally, thank you to my parents for their support and patience throughout the years.

Contents

List of Figures

List of Tables

Chapter 1

Introduction

1.1 Electrical Impedance Myography

Electrical impedance myography (EIM) is a technique developed by researchers at Beth Israel Deaconess Medical Center (BIDMC) and Northeastern University to monitor and diagnose neuromuscular diseases rapidly and non-invasively. EIM characterizes the "intrinsic architecture of muscle fibers" by measuring the muscle's effect on an alternating current [9].

EIM measures the electrical impedance of the muscle by transmitting an alternating current through the muscle and measuring the voltage generated across the muscle. The muscle can be modeled as a network of resistors and capacitors. Each muscle cell and its surrounding fluid can be modeled by the network shown in Figure 1.1. In this figure, R_1 represents the extra-cellular fluid resistivity, C_1 represents cell capacitance, R_2 represents intra-cellular fluid resistivity, C_2 represents organelle capacitance, and R_3 represents organelle resistivity.

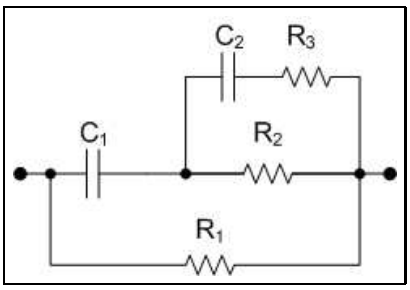

Figure 1.1: Circuit model of muscle cell.

The EIM measurement yields impedance, which is a complex number. As a complex number, the EIM measurement has two parameters: resistance, R, and reactance, X. These two parameters are used to determine the phase, θ, which is particularly useful in assessing muscle health [4]. The phase is calculated as follows:

$$\theta = \tan^{-1}(R/X)$$

EIM measurements are taken in a completely non-invasive manner, by placing electrodes on the patient's skin. At least four electrodes are used: two excitation electrodes and two pick-up electrodes. The excitation electrodes source and sink the current through the muscle, and the voltages at each of the pick-up electrodes is measured. The voltage measurement cannot be taken at the excitation electrodes instead of the pick-up electrodes, i.e., there must be four electrodes instead of two. All four electrodes are required in order to capture the voltage only across the muscle and not across the muscle and the skin and fat layers. Since the muscle is significantly more conductive than the layers above it, measuring the voltage at different electrodes than the excitation electrodes ensures that at the pick-up electrodes, all of the current is passing though the muscle. EIM measurements are independent of the thickness of the skin-subcutaneous fat layer [19]. In fact, EIM measurements taken above the skin are very similar to EIM measurements taken on surgically exposed muscle [6].

There are four common forms of EIM measurements. The most basic is **Linear EIM**, which measures the impedance of the muscle at a single frequency, usually 50kHz, while varying the distance between the electrodes along the muscle. This method is called "linear" EIM because the distance between the electrodes is varied along the same line, as in Figure 1.2. The impedance is calculated as a function of the distance between electrodes, and increases monotonically as distance increases [1].

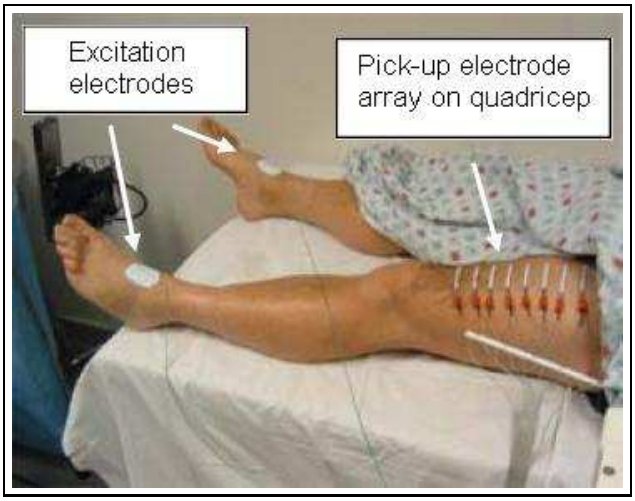

Figure 1.2: Current Linear EIM electrode array [31].

Linear EIM has been expanded to include multiple frequencies, a form aptly named **Multi-frequency Linear EIM**. Measurements obtained from Multi-frequency Linear EIM provide a more thorough characterization of the muscle in question, because different frequencies provide different information about the condition of the muscle [21]. The most useful frequencies range from 1kHz to 4MHz.

Muscle is an anisotropic medium, meaning that the muscle impedance depends on the orientation of the measurement [10]. The impedance measurements, at all frequencies, taken parallel to the muscle fibers are much smaller in magnitude and phase than the measurements taken perpendicular to the muscle fibers. In a normal, healthy muscle, the

ratio of perpendicular phase values to parallel phase values is two. In diseased or weakened muscles, however, that ratio nears one, as the EIM measurements taken perpendicular to the muscle fibers decrease in magnitude. The form of EIM called **Rotational EIM** uses a rotating electrode array to take measurements at multiple orientations.

Impedance measurements are also affected by the dynamic state of the muscle. Resistance and reactance measurements taken while the muscle is being voluntarily contracted have greater magnitudes than those taken on a relaxed muscle [8]. **Dynamic EIM** is a new concept in the realm of EIM, and it is difficult to perform due to the challenges associated with maintaining a consistent level of contraction while the measurements are being taken. Even though EIM measurements can be taken very rapidly (within a matter of seconds), the amount of muscle contraction can change significantly enough in a short time, rendering the measurements useless.

The relevance of EIM to neuromuscular diseases lies in the potential of EIM to detect changes in the health of muscles. The weakening of muscles occurs for three primary reasons:

1. Muscle atrophy or loss
2. Edema or swelling of the muscle
3. Fatty replacement of muscle fibers

Since all of these changes in muscles alter the cells that comprise muscles, they also affect the impedance measurements. Therefore, these factors that cause muscle weakening are detectable by EIM, making EIM a valuable tool in evaluating neuromuscular diseases and muscle health [4, 5]. Additionally, EIM measurements are directly related to the functional ability of the muscle. For example, certain impedance measurements directly

imply that a patient's leg muscles are strong enough for the patient to walk across the street [11].

1.2 Neuromuscular Diseases

Neuromuscular diseases whose progression can be tracked using EIM include a wide variety of disorders. Some neuromuscular diseases, called myopathies, primarily affect muscles, while neurogenic diseases are neuromuscular diseases that directly affect nerves, and thus they indirectly affect muscles as well. These disorders are often debilitating and painful, and they can lead to sensory loss and permanent disability. Additionally, they are difficult to monitor with current assessment techniques, which will be discussed in Section 1.3.

Myopathies have a number of causes. They include muscular dystrophies, inflammatory myopathies, toxic myopathies, and congenital syndromes. Some are caused by prolonged drug usage, such as corticosteroid-related myopathy. This myopathy is among the most common drug-induced myopathies. It affects 10% of patients treated with corticosteroid medication for more than 90 days [12]. Other myopathies are genetic. Duchenne muscular dystrophy is an example of such a myopathy. It affects 1 in 5,000 boys [26].

Neurogenic diseases are also fairly widespread. This group of neuromuscular disorders includes diseases that affect the entire body, such as amyotrophic lateral sclerosis (ALS), and also localized conditions such as carpal tunnel syndrome and ulnar neuropathy. These localized disorders contribute to the high frequency of neurogenic diseases. For example, carpal tunnel syndrome has lifetime prevalence of approximately 10% [14], meaning 10% of the population has suffered from this disorder at some point in their lifetime.

Disuse atrophy, which is not officially classified as a neuromuscular disease, is another muscle condition that can have dire consequences. Disuse atrophy is the loss of muscle tissue caused by prolonged disuse of the muscle [23]. For example, after a hip fracture, the patient's leg muscles are weakened because the patient must avoid use of the leg while the bone is healing.

1.3 Current Methods of Muscle Health Assessment

Assessing muscle health is a challenging proposition for health care professionals today. The most commonly used assessment techniques have not been significantly updated since the 1950s, and they all suffer from one or more of the following shortcomings: invasiveness; qualitative results instead of quantitative results; lack of reproducibility; subjectivity; dependence on patient effort.

Needle Electromyography (EMG) is the most commonly used method of muscle assessment for patients with neuromuscular diseases. Unlike EIM, which describes the electrical properties of the muscle, EMG measurements depend on the electrical activity in the muscle, i.e. EMG electrically stimulates the muscles being tested while EIM avoids doing so [9]. EMG requires the tester to qualitatively judge the attributes of motor unit action potentials (MUAPs) on an oscilloscope. To do so, the tester probes the muscles in question with needles. Each measurement session lasts approximately 20 minutes. The patient must contract the muscles against the needles; this procedure is invasive and painful. This drawback alone makes EMG undesirable, particularly for use in children. Surface EMG has been tested by clinicians, but the surface electrodes cannot sufficiently isolate the MUAPs through the skin [30]. Furthermore, even though EMG is only performed by trained professionals, there are often inconsistencies between testers [28]. Also, EMG is dependent on patient effort, making it very subjective; if a patient's

disease has progressed sufficiently to make using the muscle painful, the patient will probably not exert as much effort as they actually are physically capable of exerting. Despite EMG's prevalence in neuromuscular disease assessment, it is a severely flawed technique for monitoring neuromuscular diseases.

Magnetic Resonance Imaging (MRI) has been used for imaging the spine in patients with radiculopathy, a neurogenic disease. MRI has also been used for pinpointing biopsy sites [25]. However, MRI is expensive, and taking measurements at a number of different muscles is particularly time-consuming with MRI. Additionally, it is difficult to focus attention on a particular, small muscle, leading to errors in diagnosis.

Ultrasound has limited use in neuromuscular disease assessment. It has been used to evaluate carpal tunnel syndrome [16] and focal nerve compression syndromes [27]. However, multiple studies have shown that ultrasound is an extremely qualitative and subjective method, because even small variations in testers' measurement techniques cause large differences in data [15, 24].

Biopsy is the "gold-standard" in muscle health assessment, since it allows the tester to analyze the properties of the muscle without interference from the patient's skin or fat layers. However, it provides imperfect information because the effects of neuromuscular diseases are sometimes not evenly present throughout the muscle. Hence, a negative biopsy does not guarantee a healthy muscle. Of course, biopsies are also much more invasive and painful than any other common method of assessment.

Manual muscle tests are used primarily by physical therapists to monitor the rehabilitation progress of their patients suffering from neuromuscular diseases or injuries. The physical therapist scores the patient on a scale from 0 to 5. For example, if a patient is recovering from a hip fracture, a score of 0 would indicate that the patient cannot move

their leg at all, a score of 3 would indicate that the patient can lift their leg slightly against the resistance provided by the physical therapist, and a score of 5 would mean that the patient can walk across the street. This test is very subjective since it depends on the physical therapist's interpretation of the patient's ability to move the muscle. Also, it depends exclusively on patient effort which adds to the subjectivity of the test. Finally, it cannot isolate all muscles and muscle groups equally.

Dynamometry is also used primarily for rehabilitation purposes. The patient is required to apply force to a dynamometer. Again, this test is dependent on patient effort and only usable on some muscle groups.

Other less common methods for assessment exist as well. Blood tests and genetic screenings have been developed to aid in the detection of hereditary myopathies [29].

1.4 First Generation EIM Prototype System

EIM has been in development for nearly 10 years. Currently, Dr. Seward Rutkove of BIDMC is conducting studies using EIM to assess ALS. The EIM apparatus being used in these studies, which is shown in Figure 1.3, fills a large cart with off-the-shelf equipment, making it cumbersome to use. Additionally, Linear EIM is used, requiring the placement of a number of adhesive electrodes to the skin (Figure 1.2). As a result, taking EIM measurements is a lengthy process, lasting up to twenty minutes.

In order to consolidate the EIM apparatus and accelerate the EIM measurement taking process, Dr. Rutkove began a collaboration with Professor Joel Dawson of MIT. With Professor Dawson's involvement, a first generation prototype of a hand-held probe to take EIM measurements was developed. This prototype consists of six different components: a reconfigurable hand-held probe with the excitation and pickup electrodes, a voltage driver

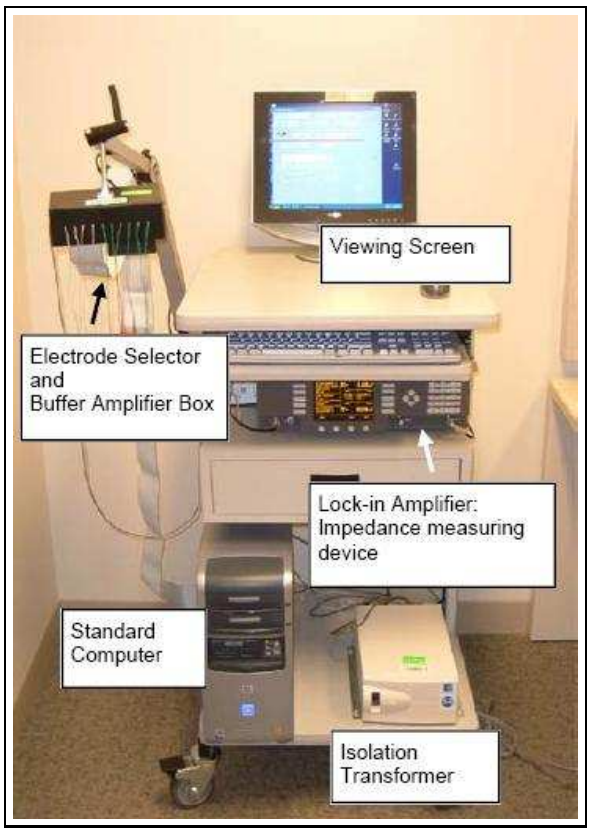

Figure 1.3: EIM apparatus currently used at BIDMC [31].

circuit, a power supply, a Tektronix AFG3102 arbitrary waveform generator (AWG), a Tektronix TDS3034B oscilloscope, and a computer. The block diagram of this system is shown in Figure 1.4. The AWG, which is programmed by the computer, sends a signal to the voltage driver circuit, which is powered by the power supply. The signal from the voltage driver is applied across the load (the muscle) by the hand-held probe, which is configured by the computer. The voltage across the load is read by the oscilloscope, and the computer reads the data from the oscilloscope and analyzes the data.

1.4.1 Reconfigurable Hand-Held Probe

The reconfigurable probe head, whose system-level block diagram is shown in Figure 1.5, consists of a CY7C68014A microcontroller, eight ADG2128 cross point switches, and an

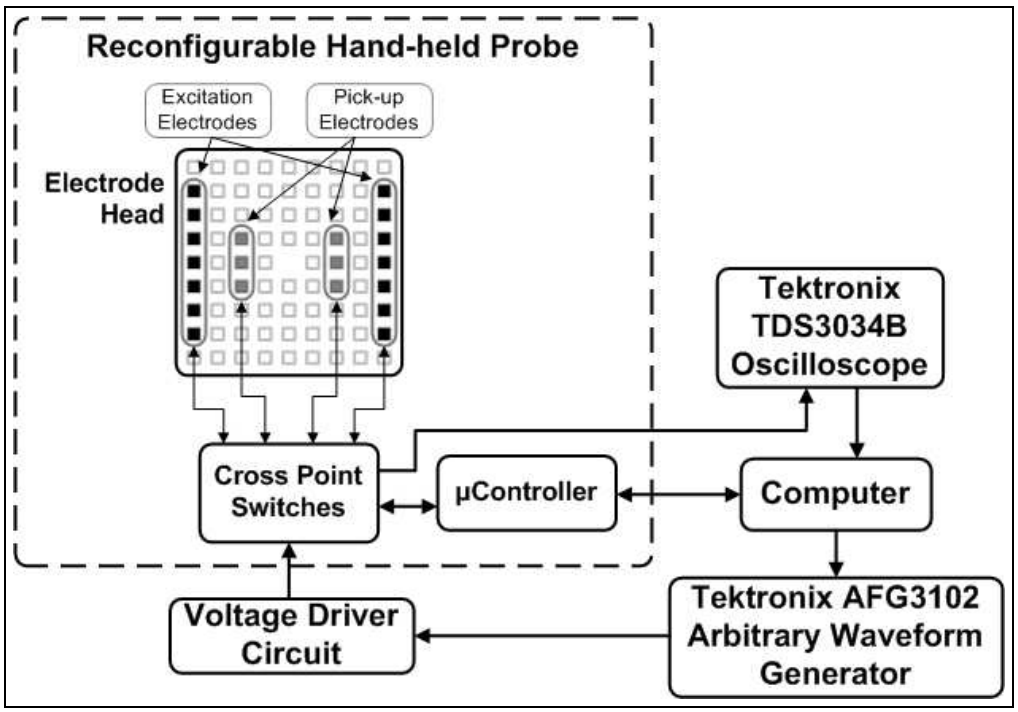

Figure 1.4: Block diagram of first prototype hand-held probe EIM measurement system.

electrode array. Each cross point switch has 12 inputs which can be connected in any combination to 8 outputs. For example, pins 4, 5, and 6 in Figure 1.6 can all be connected to pin 9. The connections are controlled by the microcontroller through a 400kbit/s I^2C interface. Of the eight outputs of the cross point switches, four are used for tetrapolar measurement taking. Pins 9, 10, 11, and 12 of Figure 1.6 are connected to the differential pickup and excitation electrodes, respectively. Using the cross point switches allows the user to reconfigure the assignment of the 96 electrode pins in Figure 1.7 almost instantly through a USB interface with the microcontroller. A GUI in Java was developed alongside the hand-held probe for reconfiguring the probe. This reconfigurability allows the user to change the orientation of the pickup and excitation electrodes without having to lift up the probe head. By avoiding replacement of the strip electrodes, this probe decreased the duration of the EIM measurement taking process. Additionally, its modular design allows for the easy replacement of differently shaped composite electrode arrays.

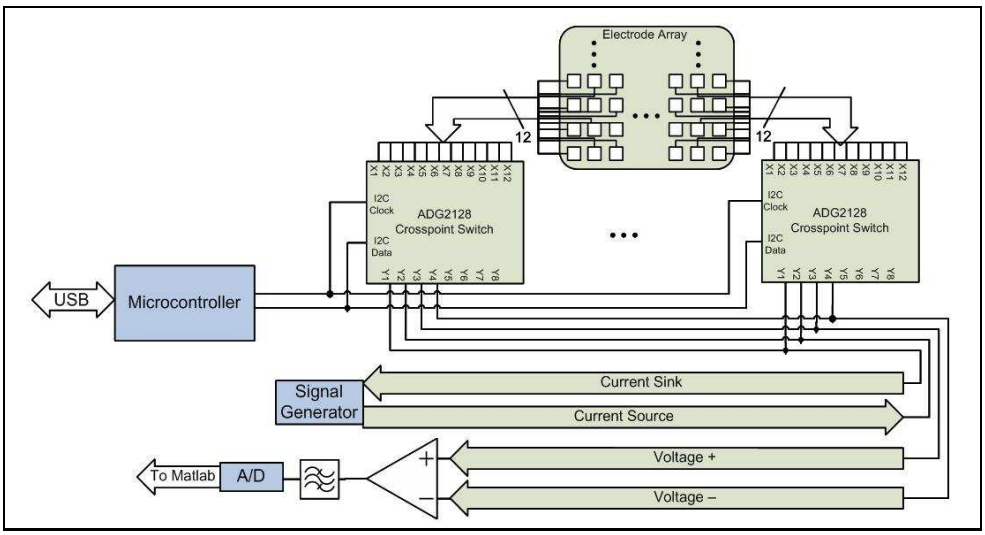

Figure 1.5: Block diagram of first generation hand-held probe [31].

This version of the probe has been tested on balsa wood and beef, two mediums which have both been shown to display sufficient similarity to the anisotropic properties of human muscle to provide reliable results [18, 20].

1.4.2 Voltage Driver Circuit

The probe injects a current driven by the voltage driver circuit into the load. The schematic of this circuit is shown in Figure 1.8. The circuit generates a purely differential voltage to minimize the common mode voltage. The load on the circuit consists of the muscle and a sensing resistor. To calculate the precise current entering the muscle, the voltage across the sensing resistor is measured and divided by the resistor's value.

Since the most useful EIM measurements are taken over a range of frequencies, the voltage driver circuit needs to produce an excitation voltage at many different frequencies. Instead of generating sinusoidal waves at the different frequencies individually, the AWG sends the sum of 35 sine waves at different frequencies to the voltage driver circuit. The 35 frequencies are logarithmically spaced over the range of 1kHz to 4MHz. The muscle

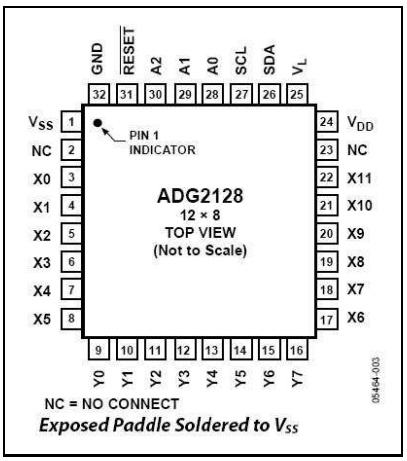

Figure 1.6: Pin configuration of ADG2128 cross point switch [13].

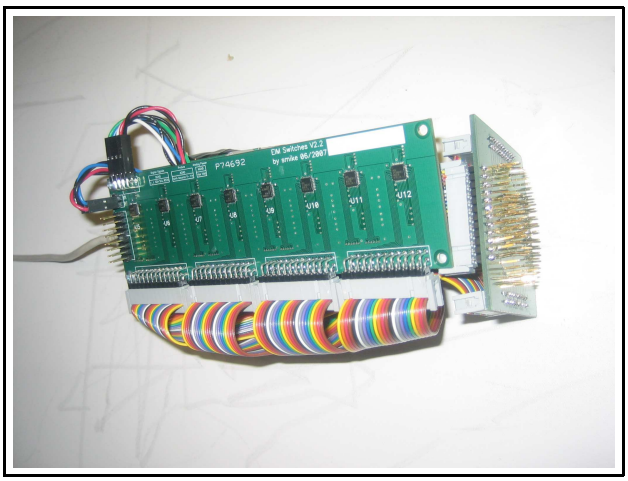

Figure 1.7: Photograph of first generation hand-held probe.

is a linear system (since it is essentially a network of resistors and capacitors), so the effect of each frequency on the muscle remains isolated when summed together. When the computer retrieves the data from the oscilloscope, it performs a Fourier transform on the data. The Fourier transforms isolate the contributions to the current and the voltage from each frequency. Figure 1.9 shows the composite signal output from the AWG. This signal is programmed into the AWG through a GPIB/USB interface to the computer.

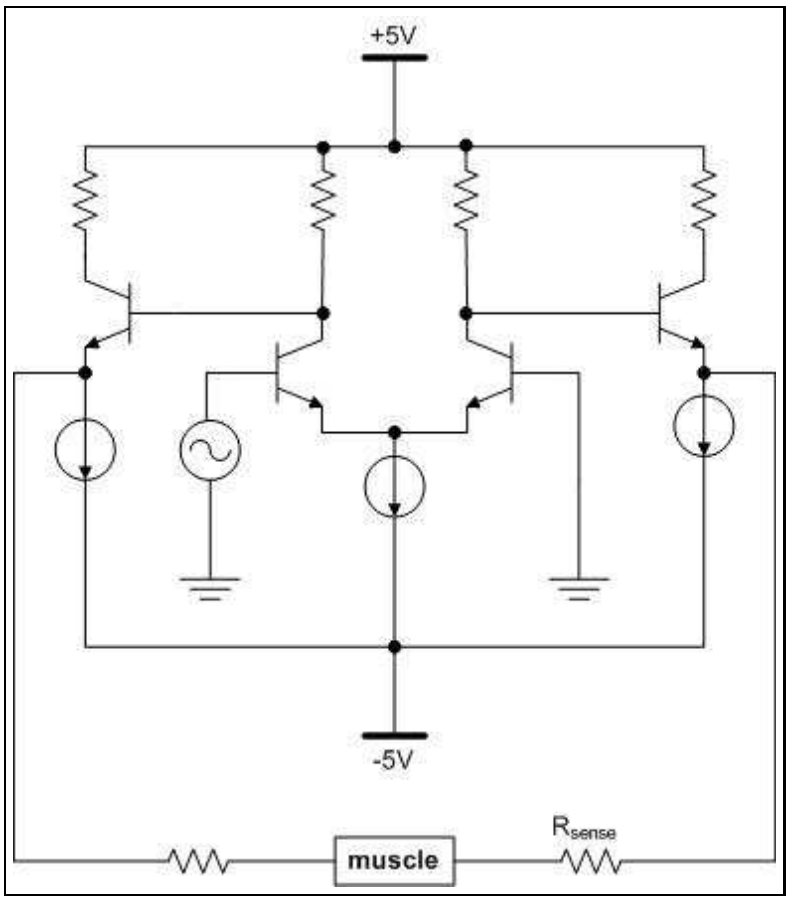

Figure 1.8: Schematic of voltage driver circuit.

The voltage driver circuit has been tested using a 5-element circuit model of a muscle, shown in Figure 1.1. The values used for the components are shown in Table 1.1.

1.5 Goals and Accomplishments

This thesis discusses improvements made to the first generation hand-held probe described in Section 1.4.1. The prototype described in Section 1.4.1 decreases the duration of measurement taking since it eliminates the need for strip electrodes. However, there are still a number of pieces of equipment and a number of software applications needed to acquire data.

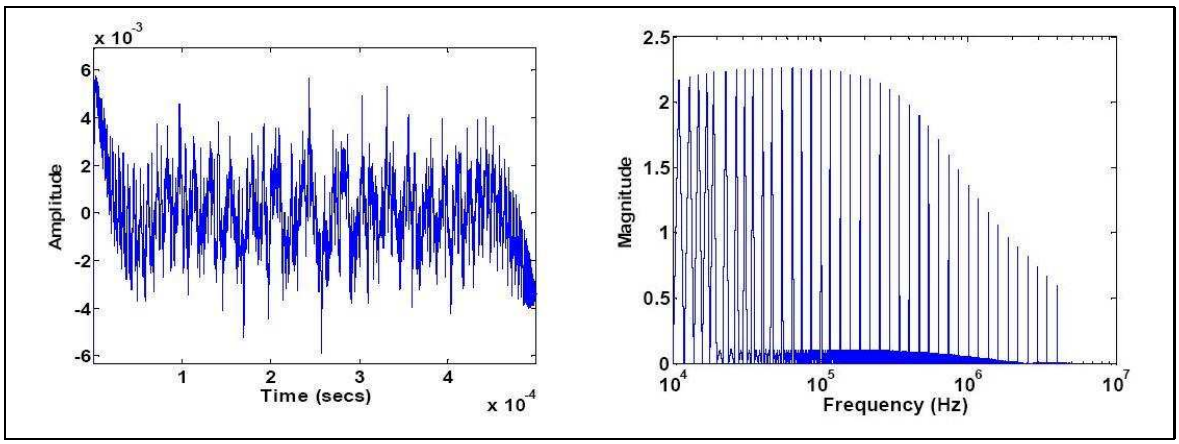

Figure 1.9: Time and frequency domain plots of the composite signal from the AWG.

Parameter	Symbol	Value
Extra-cellular Fluid Resistivity	R_1	23.0Ω
Cell Capacitance	C_1	$47nF$
Intra-cellular Fluid Resistivity	R_2	122.0Ω
Organelle Capacitance	C_2	$1.5nF$
Organelle Resistivity	R_3	150.9Ω

Table 1.1: Muscle circuit model component values.

The effects of differently shaped and sized electrode arrays on EIM measurements were examined further. Additionally, in order to simplify the user experience, a new probe was designed. This probe consolidated the first generation hand-held probe, the voltage driver circuit, and the power supply. In order to make the probe less intimidating to patients– the first generation probe had exposed circuitry, sharp corners, and sharp pins–the new probe was made flat and round, with a specially designed casing.

Also, a new graphical user interface was developed to perform all of the tasks that require the computer: programming the arbitrary waveform generator, configuring the electrodes, taking data from the oscilloscope, and analyzing the data.

Finally, preliminary exploration into further accelerating the measurement taking process was completed. The fundamental limits on measurement time were established. The measurement taking process was accelerated by taking measurements at multiple orientations simultaneously.

Chapter 2

Hardware Development

The hand-held prototype system described in Section 1.4.1 was a useful preliminary design. Modifications were made to this design to increase the flexibility and usability of the hand-held probe. New electrode heads were designed for use with the first hand-held prototype system, which validated the theory that different electrode array geometry yields similar measurements. A new hand-held probe was also designed, which consolidated separate parts of the older design.

2.1 Electrode Head Designs

In the hand-held probe, the electrode head is the circuit board that has connections to the electrode array. The electrode array is made up of a number of metal electrodes which directly touch the patient's skin (see Figure 2.1). The electrode heads of the first hand-held electrode probe are shown in Figure 2.2. These designs were a useful tool for testing the preliminary design of the hand-held probe. This hand-held probe version was designed for modularity, to allow the user to interchange different electrode arrays for different purposes. These electrode arrays were too large (∼2in) for testing on small muscles, such as those in the hand, or for testing on small animals, such as rats. Additionally, the

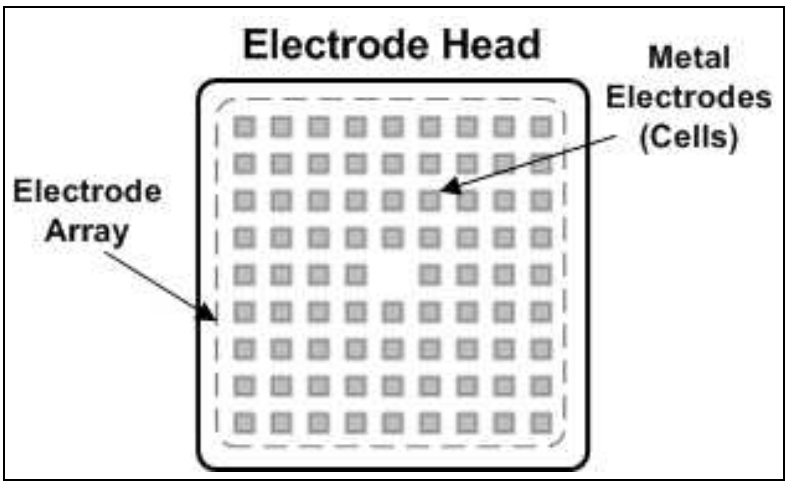

Figure 2.1: Electrode head illustration.

electrodes on the arrays made contact to the patient's skin with pins, which, although not invasive, are still uncomfortable for the patient.

The next set of electrode head designs were designed for use with rat testing. Rats provide a compromise between testing on dead muscle (beef) and expensive and risky testing on human subjects. The electrodes on these new arrays were placed closer together than the previous versions of the electrode arrays. To be exact, the new electrode arrays' electrodes were placed at half the diameter of the previous circular boards. For both versions, even though the electrode positions changed, the size of the circuit board holding the arrays was the same ($\sim$2.5in $\times$ 2.5in). For further flexibility, another board was designed, which not only had electrodes placed close together, but the circuit board itself was also much smaller ($\sim$1in $\times$ 1in).

To increase patients' comfort, alternatives to the original pin electrodes were considered. The original pins were square and pointed at the tips, so an electrode head with round pins was made. These round pins were thinner than the square pins, and the tips were rounded, ultimately making the electrode head feel much more comfortable against the

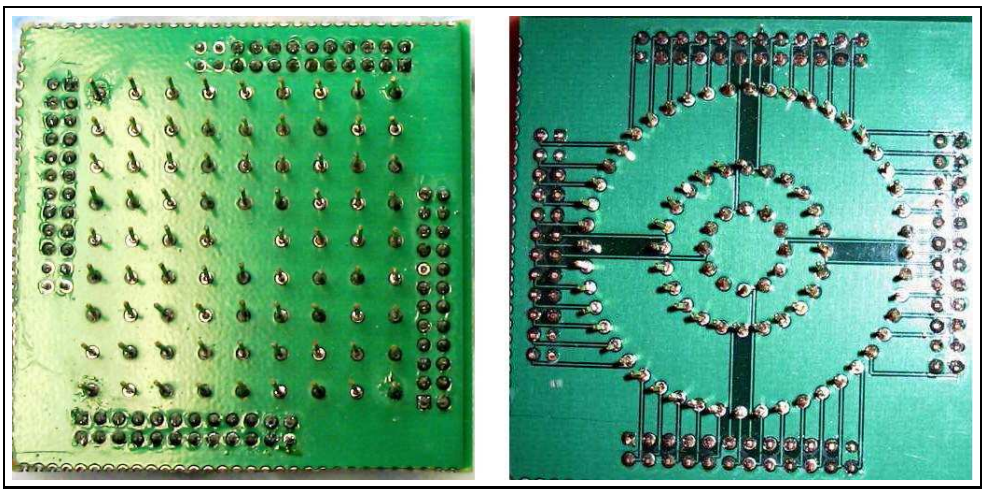

Figure 2.2: First generation electrode head designs.

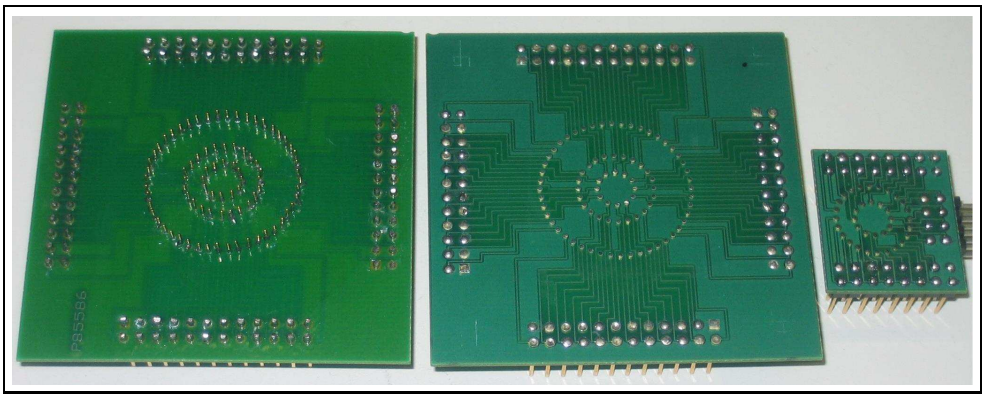

Figure 2.3: New electrode head designs (smaller, with pads and round pins).

skin. To eliminate the use of pins altogether, circuit boards were also designed for the electrode array without any pins at all. Instead, on these circuit boards, the electrodes were simply pads of copper without vias for pins drilled through them. Figure 2.3 shows some of the new heads and their relative sizes.

Measurements were taken with the new electrode heads to determine if, given the same circuitry driving the voltages, changes in electrode head geometry affect the values of the measurements. Figure 2.4 shows measurements taken on balsa wood with both the old electrode head design (larger diameter, sharp pins), and the new electrode head designs

at two different diameters.

With pins, the data in Figure 2.4 was taken with the pick-up electrodes located on the middle circle of electrodes, and the excitation electrodes located on the outer-most circle of electrodes. The distances between the electrodes were ∼2in and ∼1in respectively. With pads, the excitation electrodes were on the outer-most circle of the large head in Figure 2.3, at a separation of ∼1in, and the pick-up electrodes were on both the middle circle of electrodes and the inner-most circle. These separations were ∼0.5in and ∼0.25in respectively.

The data from the pins is close to that of the pads with the larger pick-up electrode diameter, and similar in shape to that of the pads with the smaller pick-up electrode diameter. This data implies that the geometry of the electrodes, pins or pads, does not have a significant impact on the data collected. This data shows, as expected, that the distance between the pick-up electrodes does matter; the smaller the distance between the pick-up electrodes (and hence, the smaller the amount of balsa wood, or muscle, between the pick-up electrodes), the smaller the resistance.

Data was also taken with the smallest electrode head shown in Figure 2.3, however, the electrodes were too close together to produce accurate results. The distance between the two excitation electrodes was less than 0.5in. Since the pick-up electrodes in this situation were separated by the same distance as the pick-up electrodes used in Figure 2.4 (∼0.25in), these results indicate that for use with this electrode probe, the excitation electrodes must be separated by at least one inch.

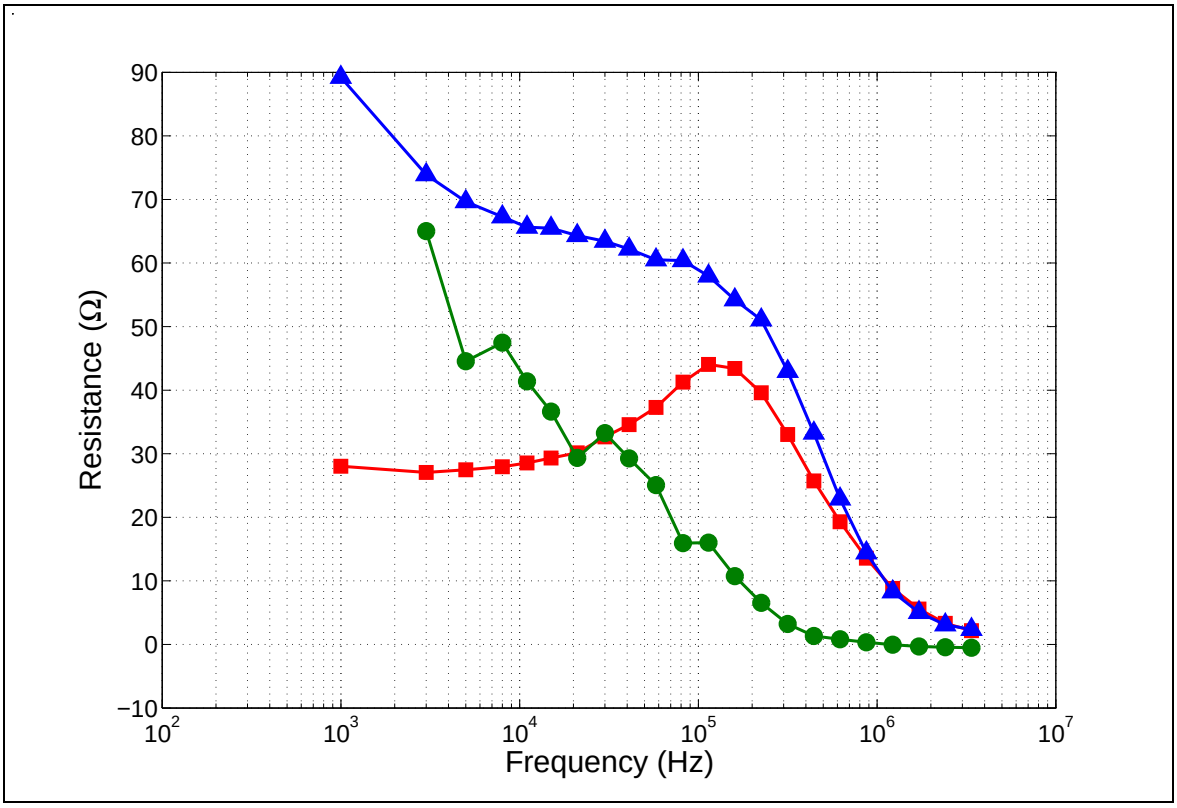

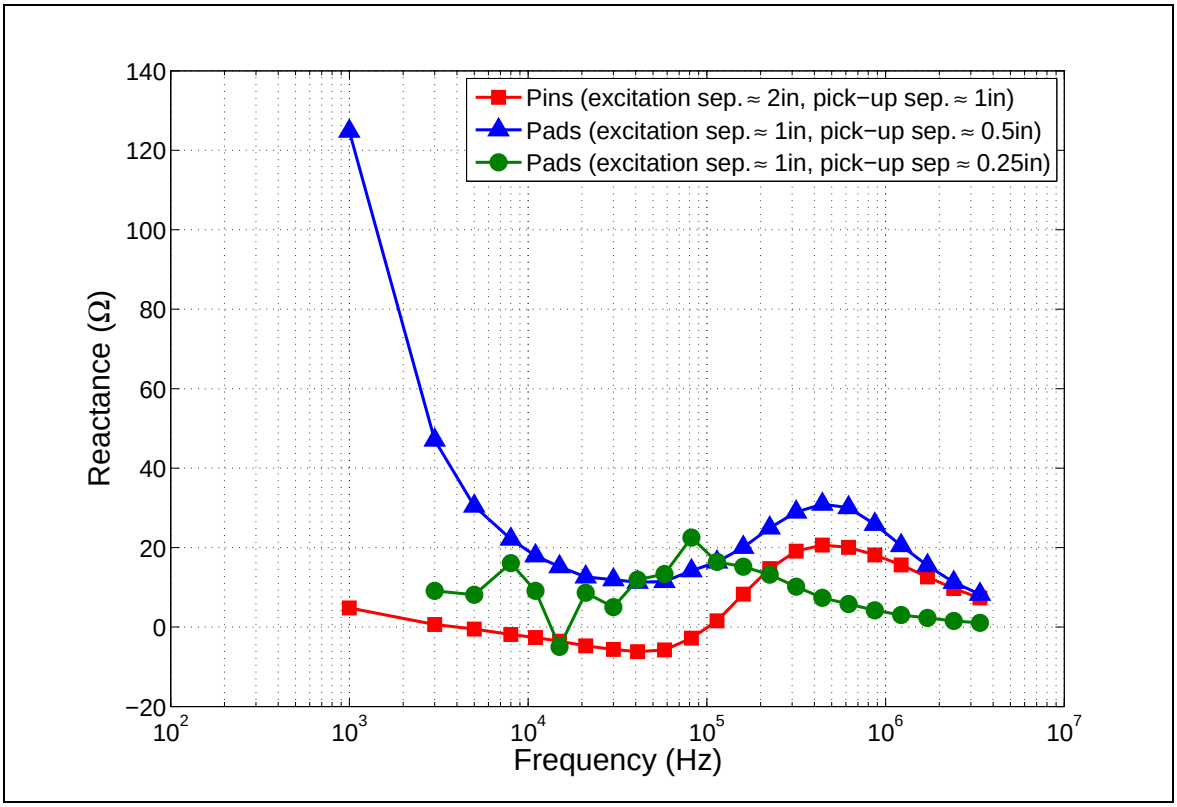

Figure 2.4: EIM measurements on balsa wood using different electrode heads.

2.2 Hand-held Probe

Once the versatility of the hand-held probe prototype was verified, the next important hurdle to pass was to receive approval for human testing from the Institutional Review Board (IRB) at BIDMC. Receiving IRB approval is necessary before the device can be tested on human subjects. The first generation hand-held prototype system could not receive approval for a few reasons. It required AC power from a power outlet to run the computer, the oscilloscope, the arbitrary waveform generator, and the power supply generating the ±5V for the voltage driver circuit, so there was a risk of power surge into the patient. Additionally, the exposed circuitry of the voltage driver circuit, the exposed circuitry on the probe itself, and the sharp corners of the probe made it undesirable for use on patients. In order to accommodate these requirements, and also to make the entire system much easier to transport between MIT and BIDMC, a number of changes were made to the system to create the second generation hand-held prototype system.

2.2.1 Control Board

The first generation hand-held system uses separate circuit boards for the microcontroller, the power supply to the cross point switches, and the voltage driver circuit. In the first generation version, only the microcontroller circuitry was on a printed circuit board. The power supply to the cross point switches used two 9V batteries and was soldered by hand onto a generic circuit board. The voltage driver circuit was assembled with discrete components on a breadboard, and required a separate external power supply. A new printed circuit board was designed and assembled which combined the digital circuitry of the microcontroller with the analog circuitry of the voltage driver circuit and the power supply. This power supply supplies ±5V to both the cross point switches and the voltage driver circuit. Figure 2.5 shows a photograph of this new board, and its schematic is shown in Appendix A.

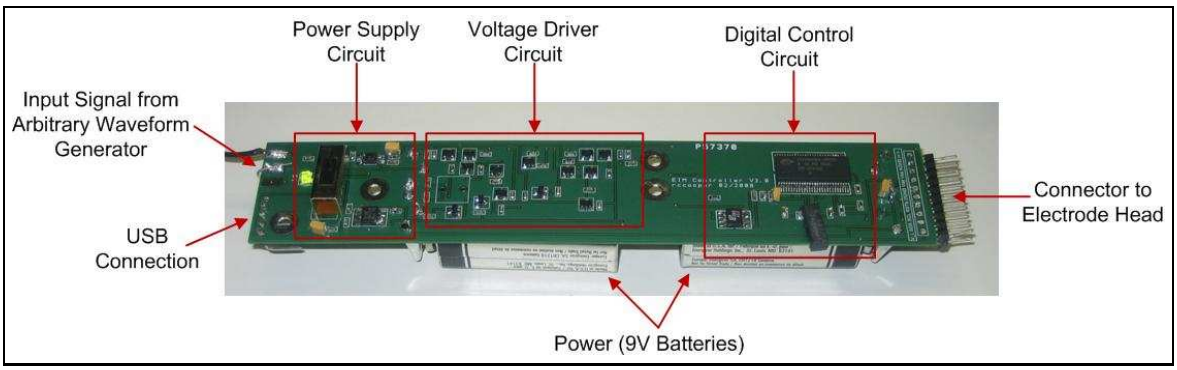

Figure 2.5: Photograph of control board.

2.2.2 Electrode Head

For the second generation prototype design, a new electrode head was designed. In the previous version, the cross point switches were on a separate board from the actual electrode head. This modularity was very convenient for interchanging the electrode heads. However, the connection between the two boards required numerous ribbon cables. These ribbon cables could easily be mixed up, causing the electrodes to be matched incorrectly with the cross point switches. The cables could also potentially affect signal integrity. In the second generation device, the electrode head was going to be specifically for human testing on a standard set of muscles, so modularity and flexibility of electrode heads was not as critical. Hence for the newest version of the probe design, the modularity of the probe was sacrificed for the convenience of having both the cross point switches and the electrodes on the same printed circuit board.

The round pattern of electrodes was selected for this version of the electrode head since it allows for the most radially symmetric data collection over the different orientations of the muscle. Since there was no need for wide ribbon cable connectors along the edges of the electrode head board as in previous designs, a round circuit board was printed. Also, since the electrode head is to be used for testing human muscles, it was made closer in size

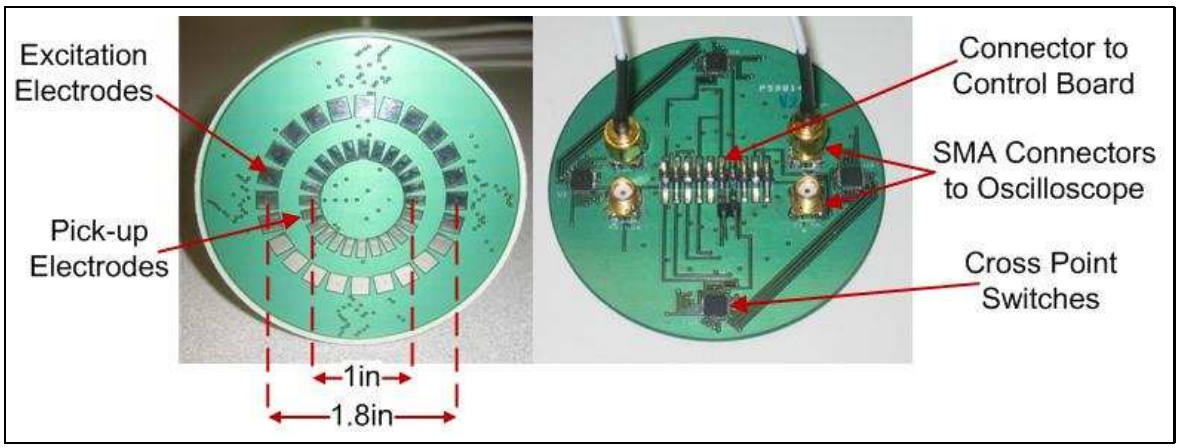

Figure 2.6: Photograph of round electrode head (top and bottom view).

to the original electrode heads. And for comparison purposes, to make the electrodes more similar to the strip electrodes used currently at BIDMC, the electrodes were widened. For optimized patient comfort, no pins were used, but only pads of copper. Based on input from Dr. Rutkove, the angular resolution of the electrode head was made to be 15°. A photograph of this electrode head from different angles is shown in Figure 2.6.

2.2.3 Other Hardware Components

Even after the new hand-held probe was designed, the oscilloscope and arbitrary waveform generator still required direct AC power. A laptop computer was used, which can be removed from AC power and run on battery power during contact with human subjects. USB from a laptop supplies some DC power (+5V DC), so an AWG and an oscilloscope that connect to the USB ports on the laptop were purchased. The TiePie Handyscope3 replaced the Tektronix AWG and TiePie Handyscope4 replaced the Tektronix oscilloscope. Figure 2.7 shows the setup with laptop, AWG, oscilloscope, and hand-held probe. This system is not completely optimized, since the AWG and oscilloscope are still off-the-shelf components, but it is a significant improvement over the first generation system in terms of both patient safety and convenience to the tester.

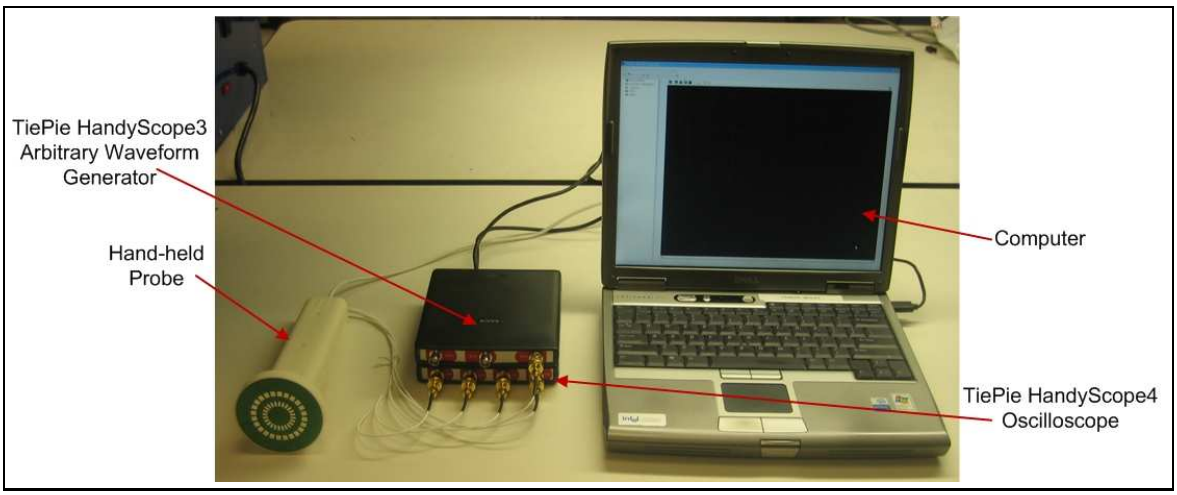

Figure 2.7: Photograph of new EIM apparatus.

Finally, it was also necessary to design a casing for the hand-held probe to protect both the circuitry and the patients. A casing was created by a fellow student using a 3D printer, and is shown in Figure 2.7.

Chapter 3

Software Development

The EIM system relies heavily on interaction with a computer: the composite signal sent to the voltage driver circuit must be programmed by the computer; the probe electrodes are configured through USB on the computer; the oscilloscope captures data and returns it to the computer for analysis; the data is analyzed on the computer. Because the interaction with the computer is such an essential part of the system, it is important to have a software system that allows the user to perform all of these tasks conveniently.

3.1 First Generation Measurement Taking Software

At the onset of research for this thesis, the software system for taking EIM measurements was tedious and complicated for new users. First, the user would have to program the arbitrary waveform generator (AWG) using code written in C++. Next, the user would configure the electrodes on the switches using the GUI shown in Figure 3.1. The next step would be for the user to open the GUI associated with the oscilloscope to capture the data (see Figure 3.2). Due to the format the GUI saved the data, the user then had to open Microsoft Excel to reformat the data. Finally, the user opened MATLAB to analyze the data. This process caused delays in the measurement taking process. On

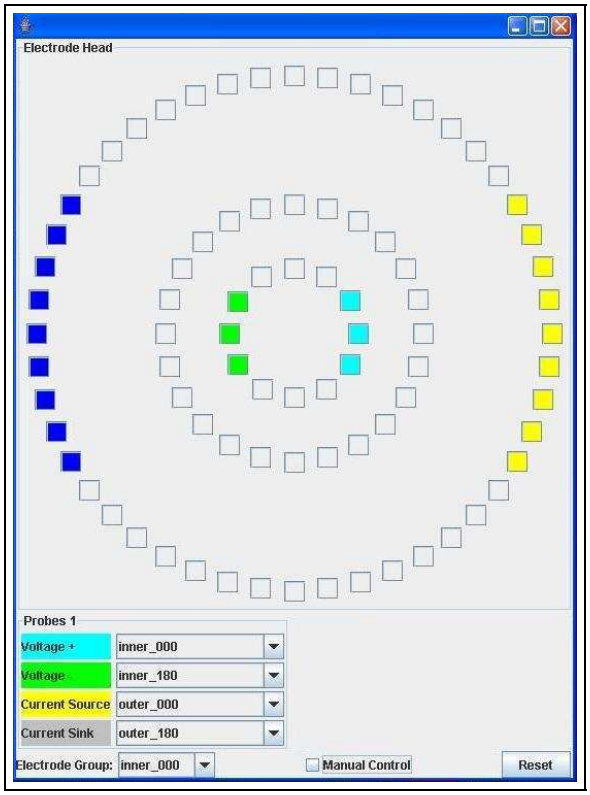

Figure 3.1: First generation electrode reconfiguration GUI.

some occasions, the balsa wood or beef being tested would dry out while the data was being taken and analyzed, causing inconsistencies in the data. This delay would be unacceptable in a clinical environment and hence the software of the EIM system had to be improved.

3.2 New User Interface: Features and Implementation

The most important requirement of the new user interface was that the GUI had to be integrated into one application. This GUI needed to be able to communicate with all of the other devices in the EIM system: the electrode probe, the arbitrary waveform

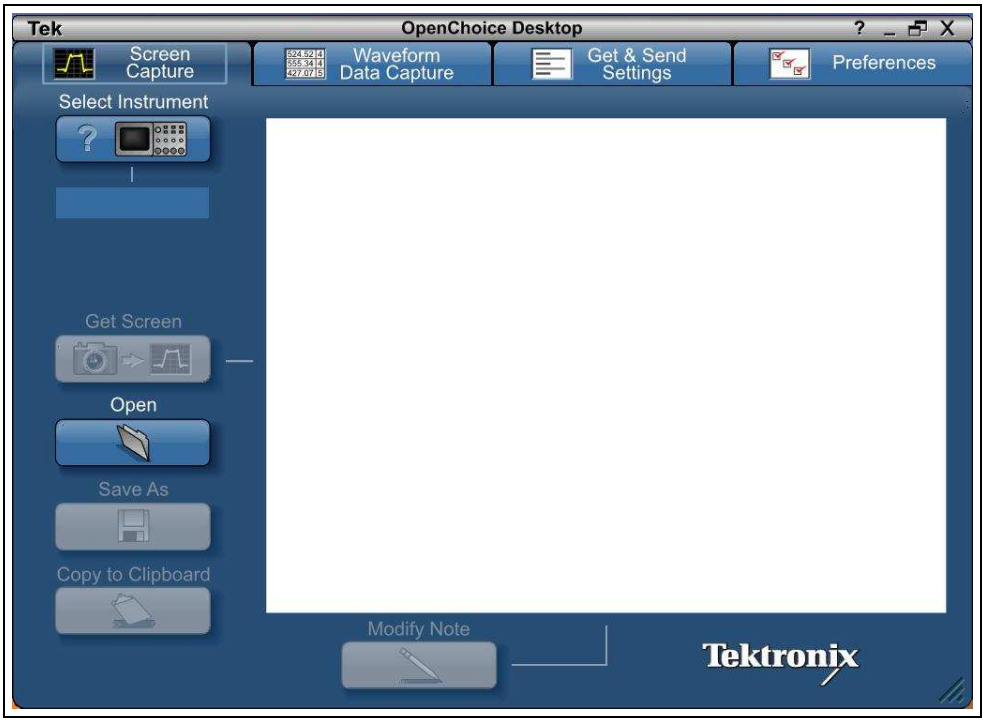

Figure 3.2: Tektronix TDS3034B oscilloscope GUI for data collection.

generator, and the oscilloscope. Additionally, the GUI had to be capable of performing sufficient data analysis to provide the user with useful information about the patient being tested.

Since the GUI is to be used by professionals whose primary focus is caring for patients–not understanding low-level software intricacies–it was necessary to develop an extremely user friendly interface. The programming language Visual Basic was chosen for this task because it was designed specifically for developing user interfaces.

Visual Basic uses "forms" and "classes" to implement code. The forms are what the user sees and interacts with, while the classes are the layers underlying the forms to execute the necessary tasks of the GUI. Each class is made up of more classes which allow for the abstraction of information. The software for the EIM system has four classes at the highest level: an electrode head controller, an AWG controller, an oscilloscope controller,

and a data analyzer. Figure 3.3 shows the class hierarchical structure for the software. Since the software will be used specifically for the EIM system, this software has captured enough of the necessary functionality of each of the individual software applications used before to provide the user with flexibility while maintaining simplicity. A screen shot of the first form that users see, which provides the most basic level of functionality, is shown in Figure 3.4.

3.2.1 Electrode Head Controller

The electrode head controller allows the user to:

1. Load the XML file that uniquely describes the current electrode head
2. Take measurements at all pre-specified electrodes
3. Specify new electrode lengths and locations
4. Monitor and control each cross point switch's inputs and outputs directly

The diagram in Figure 3.3 shows that the electrode head controller maintains lists of cells and groups. These names represent a hierarchy that must be violated in order to provide the user more flexibility. The "cells" are each of the electrodes in the electrode array. The cell structure in the code corresponds to the input pins on the cross point switches. Hence, the number of cells an electrode head has is equal to 12 times the number of cross point switches on the electrode head. These cells in software correspond to the pins or pads that touch the patient's skin in hardware. The "groups" are combinations of cells where each cell is tied to a specific function as a positive pick-up electrode, a negative pick-up electrode, a positive excitation electrode, or a negative excitation electrode. The cells and groups for a specific, physical electrode head are specified using a particular format in an XML file, an example of which is shown in Appendix B.

Figure 3.3: Hierarchical class structure for EIM software in Visual Basic.

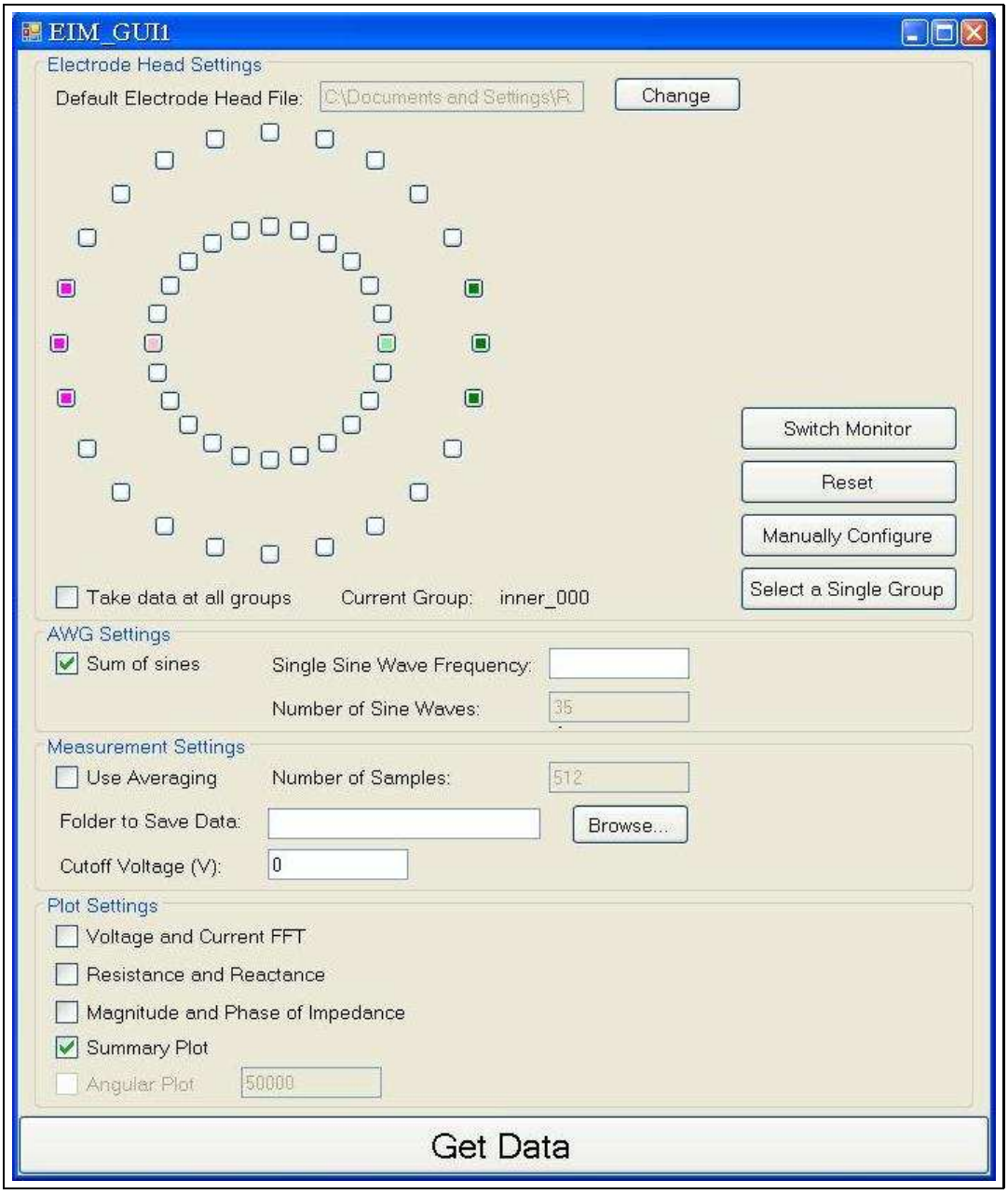

Figure 3.4: Screen shot of graphical user interface.

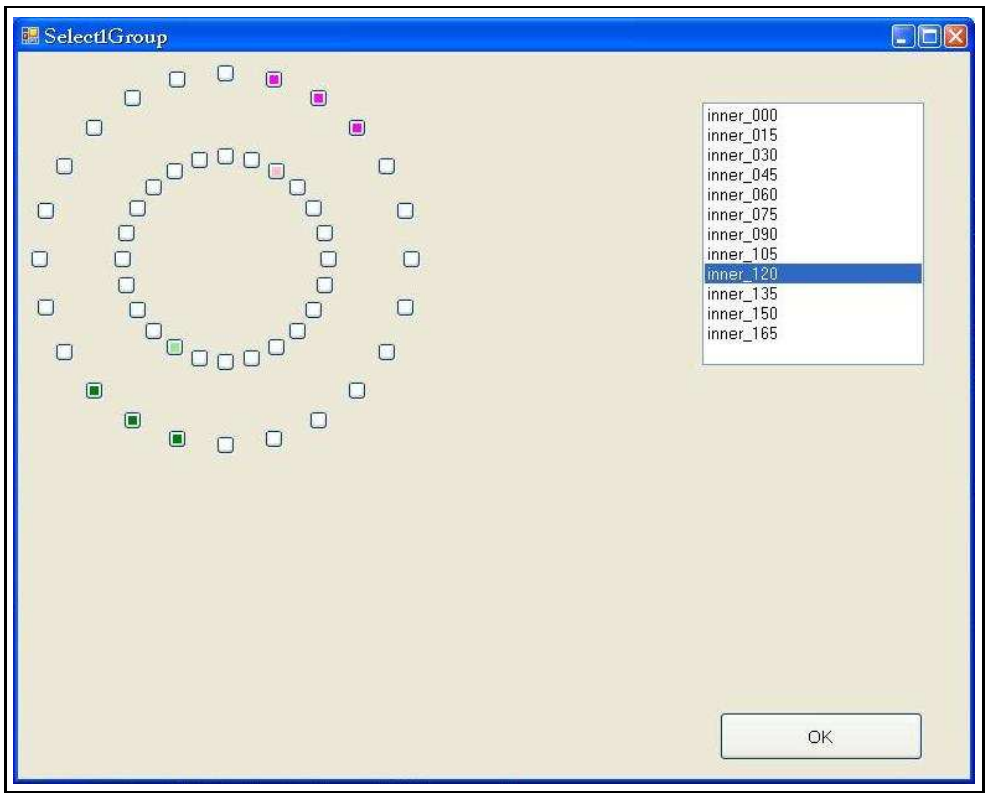

Figure 3.5: Screen shot of single group selection form.

When the software loads the user-specified XML file, by default it takes measurements at each of the groups specified in the file. Since each group represents a different orientation for the electrode heads made thus far, it will generally be useful to take measurements at each group. However, when the user wants to focus on a particular orientation, they are able to specify a particular group at which to take data. The user selects a specific group in a separate form, which is shown in Figure 3.5, which is accessed from the initial form. Furthermore, if a user wants to configure the electrode head with a set of pick-up and excitation electrodes not pre-specified by the XML file, the software allows the user to individually select cells to make up each pick-up and excitation electrode. In order to allow the user to control the electrode head on these different levels, the abstraction barrier between the cells and groups must be crossed.

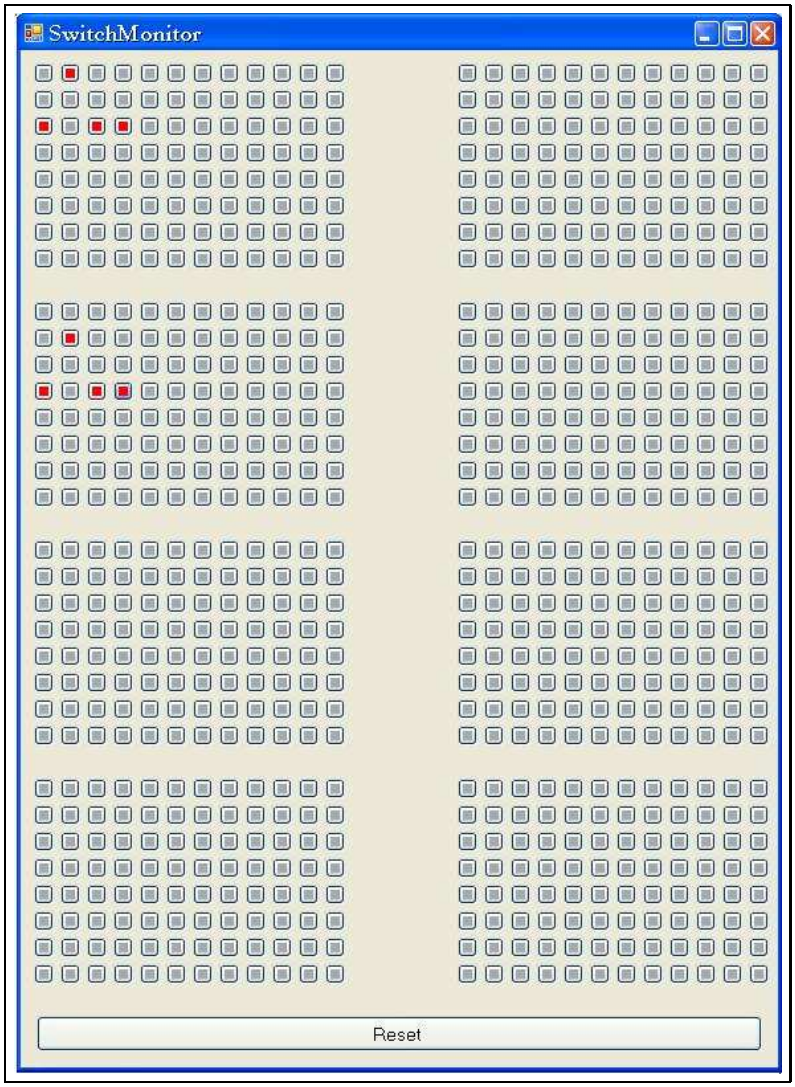

Figure 3.6: Interface for monitoring cross point switch states.

Occasionally, primarily for the purposes of debugging, it will be useful for the user to see which connections of each of the cross point switches are turned on. Figure 3.6 shows this feature of the software. The red boxes are the connections between the inputs of the cross point switches (the columns) and the outputs of the cross point switches (the rows).

When the user begins data collection, the software initiates a communication with the microcontroller that controls the cross point switches of the device. The communication

occurs using the libusb-win32 libraries for interfacing with the USB. The software communicates with drivers and firmware written for the previous version of the microcontroller.

3.2.2 Arbitrary Waveform Generator Controller and Oscilloscope Controller

TiePie, the company which manufactures and sells the AWG and the oscilloscope, provided a DLL library for easy control of the AWG and oscilloscope through a programming language. The AWG controller class creates a signal which is either a single sine wave or the sum of sine waves. The signal must be exactly 65536 samples long to fill exactly the size of the memory in the AWG allocated for arbitrary signals. This signal is set to have an amplitude appropriate for the voltage driver circuit (100mV). This signal is then placed into an array which is passed to the AWG. Due to an incompatibility with Visual Basic and the DLL provided, the actual passing of the signal occurs in a specially-written C++ program called by Visual Basic.

The oscilloscope controller uses the DLL functions to ensure that the oscilloscope is ready to take a measurement and then it retrieves the data. The data collected by the oscilloscope is in the form of four arrays of voltages, of 65536 samples each. The sampling frequency of the oscilloscope is set to 50MHz with 12-bit resolution. The arrays obtained correspond to the voltage at the positive pick-up electrode and the negative pick-up electrode, and to the voltages across the sensing resistor, called positive and negative sensing voltages. The oscilloscope controller saves the data collected into a comma delimited (csv) file and saves the file in a folder specified by the user. This allows the user to have access to the actual raw data in the event that further manipulation of the data becomes useful.

3.2.3 Data Analyzer

The data analyzer allows the user to glean information from the data collected by the EIM system. The oscilloscope controller passes the data to the data analyzer in four arrays of voltages. The arrays correspond to positive pick-up voltages, negative pick-up voltages, positive sensing voltages, and negative sensing voltages. The differential voltage between the pick-up electrodes, i.e. the voltage generated across the muscle, is calculated by taking the difference of the positive and negative pick-up voltage arrays. The current through the muscle is calculated by finding the voltage across the sensing resistor, i.e., the difference between the array of positive sensing voltages and the array negative sensing voltages, and dividing by the value of the sensing resistor.

Once the voltage across the muscle and the current through the muscle have been measured, the impedance of the muscle can be calculated. Since the current transmitted through the muscle has many frequencies, the frequency components of the voltage and on the current must be isolated. Hence, Fourier transforms are performed on the voltage and current at this stage. A radix-2 Cooley-Tukey Fast Fourier Transform algorithm is used [17]. This algorithm uses decimation in time and combines the discrete Fourier transforms (DFTs) of the even and odd numbered indices of the input signal.

Let the input signal be x, with length N samples. The algorithm requires that N be a power of 2. Let $M = N/2$, $m = 0, 1, 2, ..., M-1$, and $j = 0, 1, 2, ..., M-1$. Let the DFT of the even-numbered samples x_{2m} be $E[j]$ and the DFT of the odd-numbered samples x_{2m+1} be $O[j]$. Then the DFT X of x is

$$X[k] = \begin{cases} E[k] + e^{-\frac{2\pi j}{N}k} O[k], & k < M \\ E[k-M] - e^{-\frac{2\pi j}{N}(k-M)} O[k-M], & k \geq M \end{cases}$$

An implementation of this algorithm is shown in Appendix C [32]. Conveniently, the length of each array returned from the oscilloscope is exactly a power of two, so no zero-padding needs to be implemented.

After the data analyzer has calculated the Fourier transforms of the voltage and current, the impedance at each frequency is simply the division of those two values. Sometimes unnecessary noise is generated from the calculations. To avoid having noisy impedance measurements present in the displayed data, the user can input a cutoff value for the Fourier transform of the current. Any impedance values generated from values of the current Fourier transform which fall below the cutoff will be ignored.

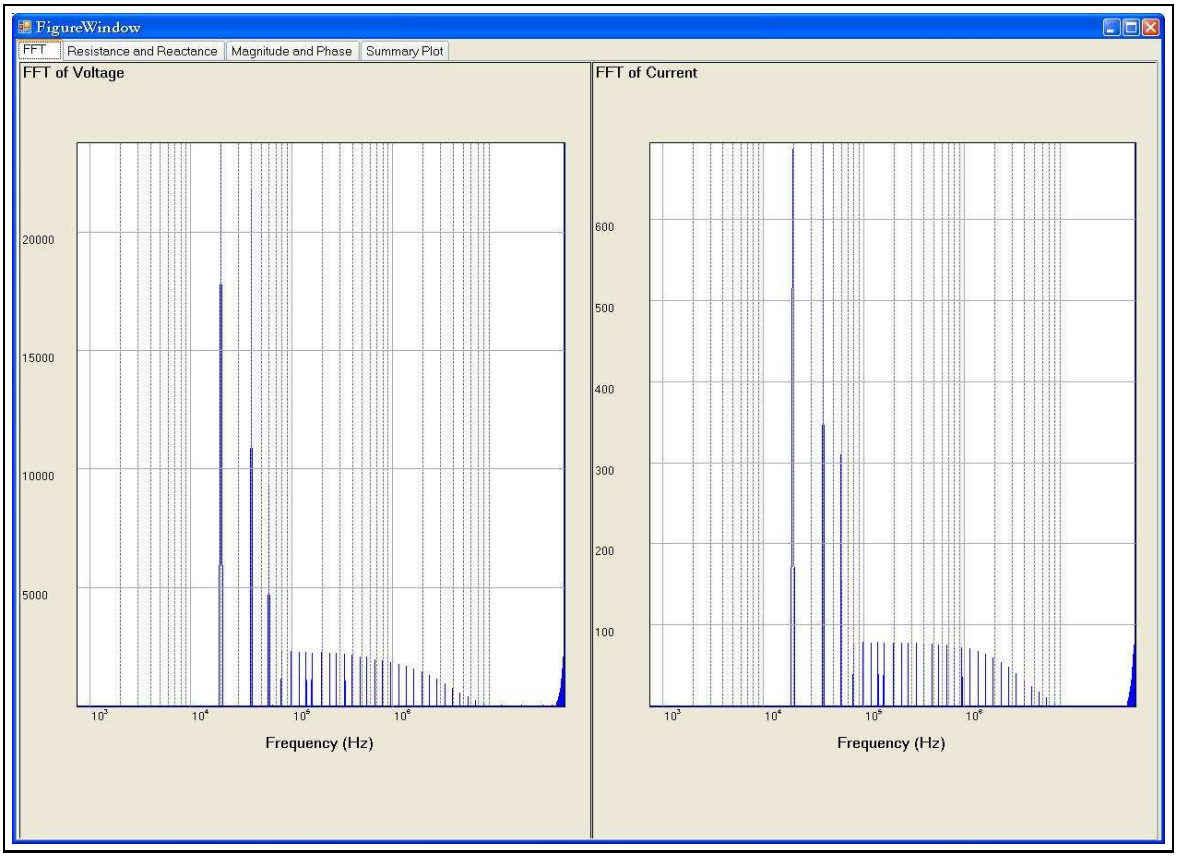

Figure 3.7: Screen shot of voltage and current Fourier transforms figure.

Based on user preferences, the impedance information is displayed to the user in a variety of plots:

1. Magnitudes of the voltage and current FFTs. This is especially helpful for determining how to adjust the cutoff value (see Figure 3.7).

2. Magnitude and phase of the impedance.

3. Resistance and reactance of the muscle, which are the real and imaginary parts of the impedance respectively.

4. A summary plot with each of the above three plots consolidated into one window.

Chapter 4

Future Work

EIM will become an indispensable tool in the diagnosis and monitoring of neuromuscular disease, but not before certain challenges are met. This chapter details the next steps to take to help establish EIM as the most common and useful method of neuromuscular disease assessment. These steps will increase the speed of the measurement taking process, decrease the amount of equipment associated with the process, and prove more extensively the accuracy of EIM.

4.1 Improved Robustness

The next phase of development and verification for the EIM device will be clinical testing. In this phase, the device will be used primarily by health care professionals, not electrical engineers, so it is critical that the device be extremely robust. The version of the hand-held probe described in Section 2.2 is more robust than its predecessor because of the plastic casing protecting the circuitry. However, special considerations regarding the design and assembly of the hand-held device must be implemented in order to achieve even better robustness.

4.1.1 Power Supply Circuit

The power supply circuit on the control board uses regulators which have power supplied to them constantly and can be turned on and off using a special enable input. While this feature can be useful, the +5V regulator turns on after the -5V regulator because it has an internal 220ms delay. As a result, the transistors in the voltage driver circuit begin to bias before both supplies are fully turned on. This premature biasing is a problem because the voltage driver circuit is purely differential, and so the relative ground begins to float. The output voltage of the +5V regulator becomes higher than its input voltage with respect to this floating ground. Hence the +5V regulator shuts off. Temporarily, this problem was solved by intentionally slowing down the -5V regulator with large capacitors. In the next iteration of the hand-held probe, the regulator circuitry should be redesigned to avoid dependence on the enable pin.

4.1.2 Mechanical Stress

The circuitry uses surface mount components, some of which are awkward to solder by hand onto the circuit boards. Baking the components in an oven with solder paste is not always a safe option as some components are not designed for such high temperatures. Due to this difficulty in soldering, some of the contacts between the components and the boards are tenuous, particularly those with the cross point switches, the microcontroller, and the surface mount SMA connectors to the oscilloscope. After a few uses, due to mechanical stresses on the boards and the connectors, the connections become unpredictable, preventing accurate measurements. For future robustness, it will be necessary to develop either new methods of soldering or new board designs to strengthen contact.

4.1.3 Integrated Circuit Development

The current EIM system requires a hand-held probe with a computer, an arbitrary waveform generator, and an oscilloscope. In order to increase the robustness, and the usability, of this device, the circuitry on the hand-held probe will be integrated onto a silicon chip. In addition to this circuitry, the integrated chip will also have a RAM that stores the composite signal generated by the arbitrary waveform generator along with a digital to analog converter, and it will also have an analog to digital converter that will be used to transmit the voltages at the electrodes to the computer. This new integrated circuit will still provide a modular design which will allow users to use electrode arrays of different shapes and sizes. It will also make the entire system much easier to use, since the system will now consist of only a hand-held probe which communicates through USB to a computer. Additionally, integrating the circuitry will help to improve the signal quality and hence the accuracy of EIM measurements. This improved accuracy will occur because the integrated circuit will eliminate parasitic effects of the discrete components.

4.2 Faster Measurement Taking Process

The first generation hand-held prototype system for EIM measurement taking in Section 1.4.1 is already a significant improvement on the current system being used for clinical testing in terms of speed. However, an even faster measurement taking process would provide further improvement to the system. When measurements are taken quickly, that reduces the risk of a change in the environment, such as temperature or humidity, which might affect the measurement. More importantly, it reduces the risk that the muscle position and contraction change during the measurement. Preliminary work was done to determine the minimum time interval necessary for measurement taking and decreasing total measurement time by taking measurements at multiple orientations simultaneously.

4.2.1 Fundamental Minimum Time Limit

Currently, the data analysis of the EIM system relies on the Fourier transform. The resolution of a Fourier transform depends directly on the number of samples taken. The Fourier transform groups the possible frequencies into ranges. For example, for data with 65536 samples and a sampling frequency of 50MHz, the frequency resolution is

$$\frac{50\text{MHz}}{65536 \text{ samples}} = 763\text{Hz}.$$

Hence any two frequencies in the composite sine wave signal that are closer than 763Hz cannot be differentiated. For example, 1000Hz and 1001Hz would fall into the same range of frequencies and would appear to produce only one contribution to the impedance.

This relationship between the number of samples and minimum frequency separation can be examined further and developed into a relationship between the length of a sample and the minimum frequency separation. Let T be the length, in seconds, of the sample and N the number of samples acquired. Let f_A and f_B be two adjacent frequencies (in Hz) in the composite signal. Finally let $\Delta f = |f_B - f_A|$ be the minimum frequency separation. Then, in order to successfully differentiate between f_A and f_B,

$$\exists k_A, k_B \in [0, N-1] \text{ such that } f_A = \frac{k_A}{T} \text{ and } f_B = \frac{k_B}{T} \text{ and } |k_B - k_A| > 1$$

For simplicity, assume that $f_A < f_B$ (the same analysis applies for $f_B > f_A$). The last constraint on k_A and k_B guarantees that f_A and f_B will fall into different frequency "buckets" after the Fourier transform is calculated. The indices k_A and k_B must be separated by at least one more index, for example index $k_C \in [0, N-1]$ where $k_C = k_A + 1$. That index must correspond to an unrepresented frequency, i.e. the discrete Fourier transform at k_C/T must be equal to 0. If the constraint were $|k_B - k_A| \geq 1$ instead,

then there would be no such index k_C, and the contributions from k_A and k_B might still overlap. Then taking the minimum separation,

$$\begin{aligned} k_B - k_A &= 2 \\ f_B T - f_A T &= 2 \\ (f_B - f_A) \times T &= 2 \\ \Delta f \times T &= 2 \end{aligned}$$

Therefore,

$$\boxed{\text{minimum frequency separation (Hz)} \times \text{sample length (s)} = 2}$$

This constraint provides insight into the tradeoff between the minimum frequency separation and the length of the sample. The constraint will be useful in the future for refining the composite signal. By changing the spacing of the 35 frequencies, the length of the sample can decrease. Studies can also be conducted to reduce the number of frequencies to just enough frequencies that still provide sufficient useful information. Or the number of frequencies can be selected in such a way to meet a strict time requirement when performing dynamic EIM.

4.2.2 Simultaneous Measurements at Multiple Orientations

EIM measurements at multiple orientations provide very important information, and a separation of 15 degrees between orientations is desirable. This separation requires measurements to be taken at $180°/15° = 12$ orientations. With the current system, each orientation is measured in series. Taking measurements at more than one orientation simultaneously will decrease the measurement time, which, as described above, is desirable.

Since muscle is a linear system, superposition of different signals in space is possible. It was hypothesized that it would be possible to take measurements at multiple orientations simultaneously if the current transmitted at each orientation was made up of a different set of logarithmically spaced frequencies. Figure 4.1 shows the setup to test two orientations simultaneously. There are two input voltages, that is, two different signals that are sent through two separate voltage driver circuits. As a simple example, consider the situation where

$$\begin{aligned} v_{IN\_A} &= V_A \sin(\omega_A t) \\ v_{IN\_B} &= V_B \sin(\omega_B t) \\ \omega_A &\neq \omega_B \end{aligned}$$

The user specifies V_A and V_B. Then, since muscle is a linear system,

$$v_B = V_{BA} \sin(\omega_A t) + V_{BB} \sin(\omega_B t).$$

V_{BA} is the contribution to v_B from the input v_{IN_A}. V_{BB} is the contribution to v_B from the input v_{IN_A}. The impedance across the muscle at ω_B is simply

$$Z_{\omega_B} = \frac{V_{BB}}{I_B}$$

Where I_B is the current through the sensing resistor at ω_B:

$$I_B = \frac{V_B}{R_{sense}}$$

The measured quantity V_{BB} is easy to obtain by taking the Fourier transform of v_B.

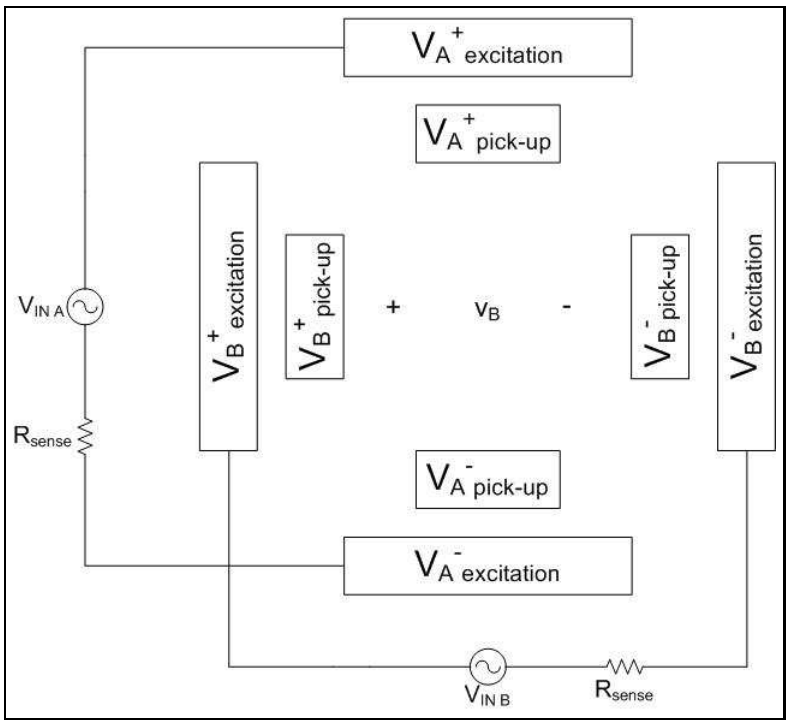

Figure 4.1: Masurement setup for two simultaneous measurements.

Preliminary experiments were conducted on balsa wood with strip electrodes to validate the claim that measurements could be taken simultaneously at two orientations. The new prototype system could not be used for these tests because of the electrode head design, but could be easily adapted in future versions for simultaneously measuring two orientations.

Measurements were taken with one set of the strip electrodes placed parallel to the wood grain ("0 degrees") and a second set forming an angle of 105 degrees from the grain (see Figure 4.2). In order to prove the linearity of the balsa wood further, with the measurements taken at angles closer to each other, measurements were also taken forming an angle 15 degrees from the grain and 75 degrees from the grain (see Figure 4.3). In both cases, as expected, the measurements taken with only one excitation voltage, and the measurements taken with two excitation voltages are almost identical.

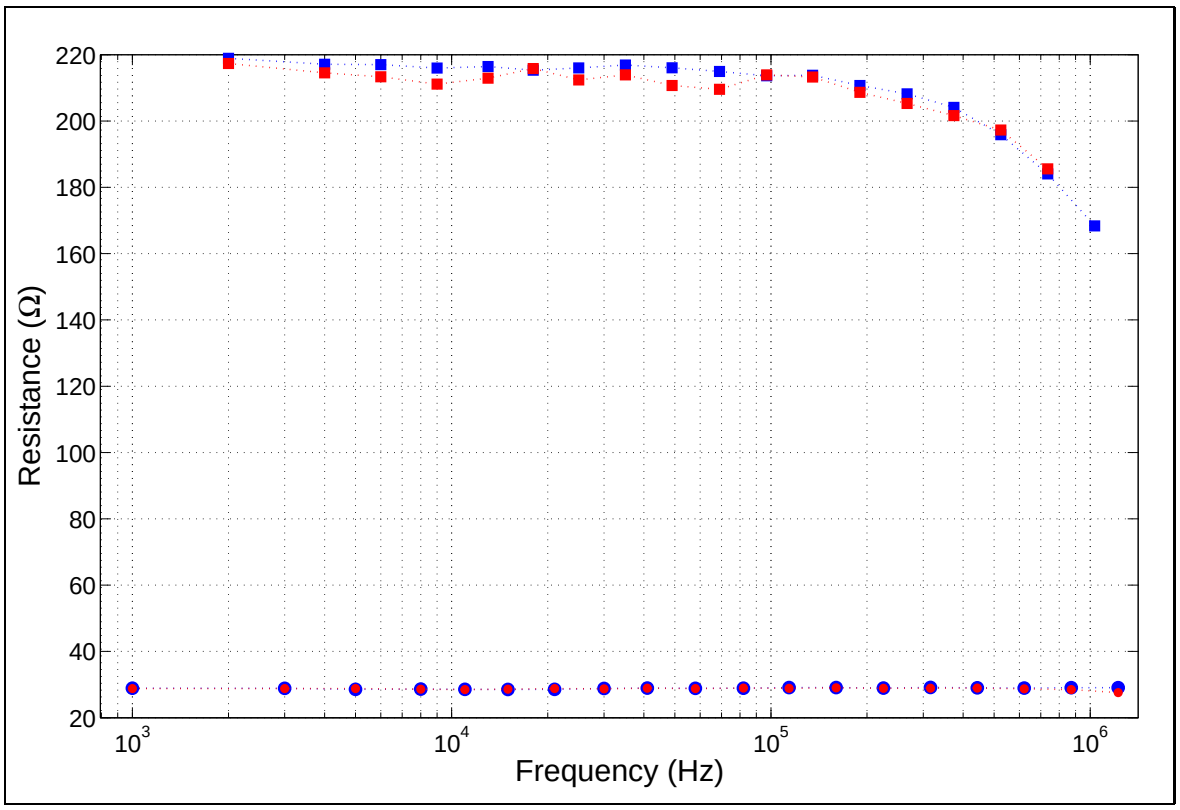

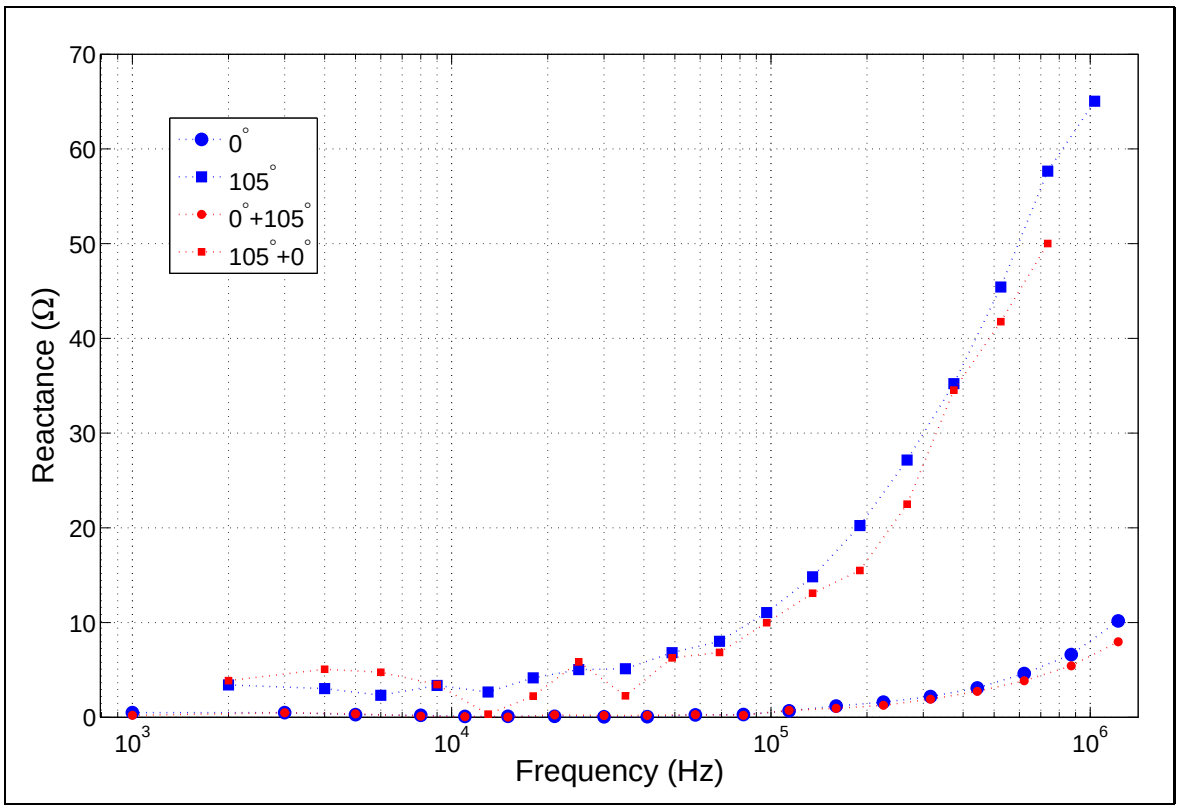

Figure 4.2: Data from simultaneous measurements at two orientations (0° and 105°).

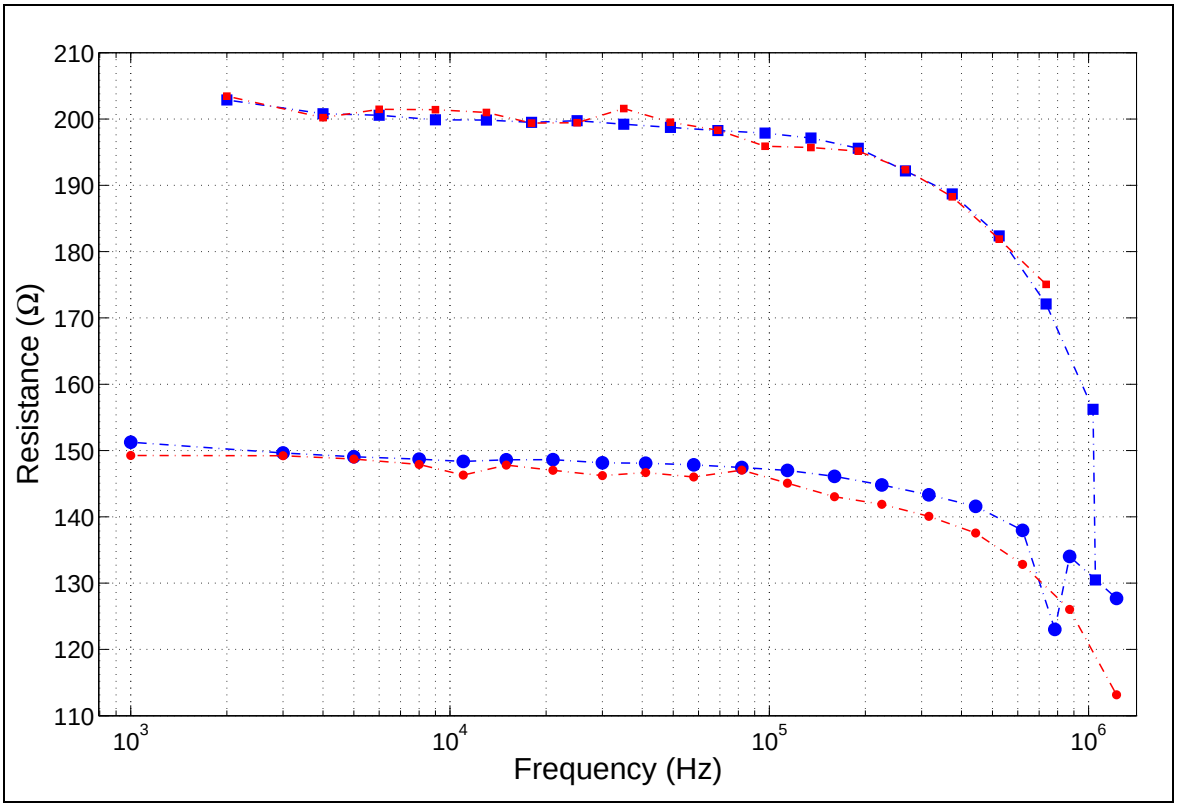

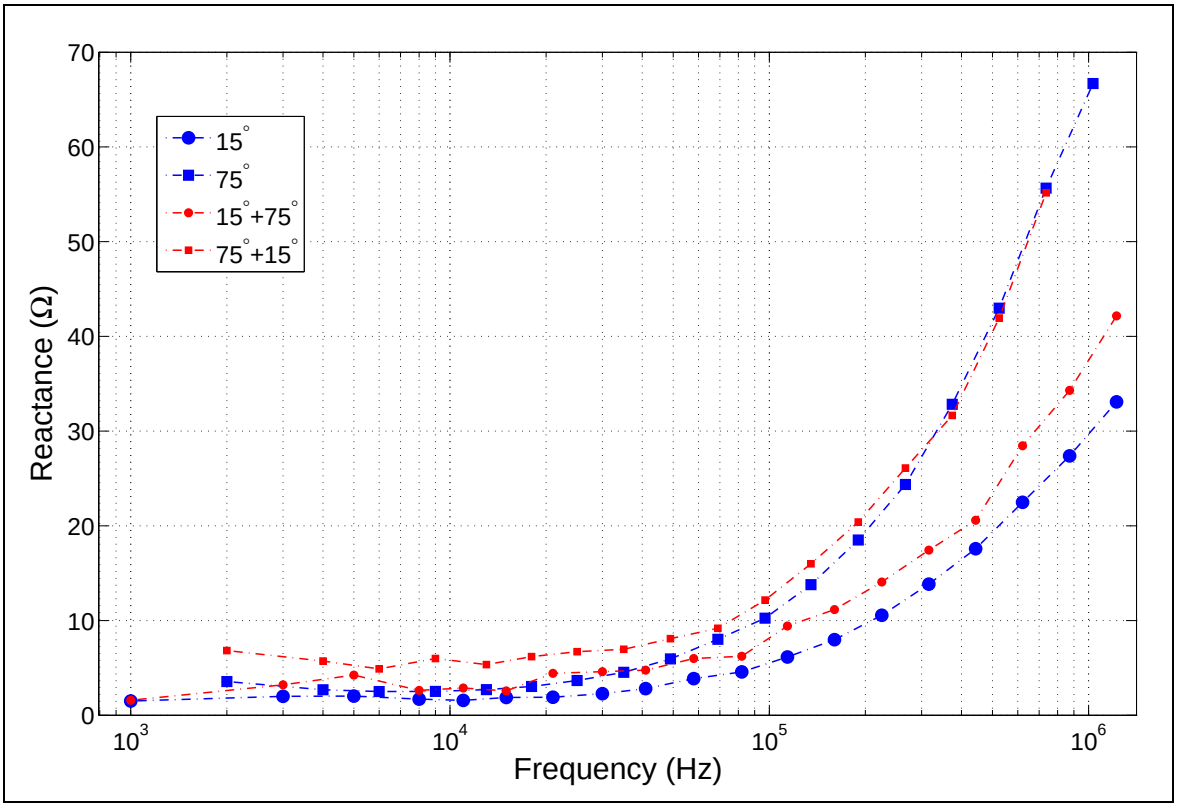

Figure 4.3: Data from simultaneous measurements at two orientations (15° and 75°).

4.3 Clinical Studies

The concept of EIM has already been proven useful through a number of clinical studies [3, 4, 5]. However, these studies have all been very focused on particular neuromuscular diseases, and they have all been completed using the old EIM system from Figure 1.3. Before EIM can achieve widespread acceptance and prevalence as a reliable tool for assessing muscle health, it will be critical to conduct more clinical studies on humans with the new hand-held device. These studies will be more extensive and exhaustive than previous studies to ensure that sufficient data has been collected to prove EIM's accuracy and safety to even the most skeptical of users.

Chapter 5

Conclusion

This thesis presents a consolidated measurement tool for the assessment of neuromuscular disease. Electrical Impedance Myography is a quantitative, objective, and non-invasive technique for assessing muscle health by measuring the electrical impedance of muscles. The current system for taking EIM measurements is bulky, with many off-the-shelf components. It also requires lengthy measurement sessions for each muscle in question, because individual electrodes must be placed at numerous locations on the skin. As a result, EIM is not yet a widely used technique for muscle health assessment.

The first generation hand-held prototype EIM system described in Section 1.4.1 began the process of equipment consolidation and consisted of a large oscilloscope, arbitrary function generator, and power supply, as well as a laptop, a hand-held probe with reconfigurable electrodes, and other circuit boards. The subsequent version of the EIM system that was developed comprised a smaller oscilloscope and arbitrary waveform generator, a laptop, and a hand-held probe with all of the additional circuitry. Additionally, new shapes and sizes of electrode heads were created to provide the flexibility to test different types of muscles. These electrodes had pins and pads which made contact with the skin, and ranged in separation from 0.25in to 2in. For these different types of electrodes, the

measurements taken were very similar, so consistency would be achievable with different electrodes, for example electrodes that have comfortable pads instead of pins.

To make the EIM system still easier to use, new software was written. This new graphical user interface combined the functionalities of a number of different applications that the user had to navigate previously. This new GUI can set the arbitrary waveform, get the data from the oscilloscope, analyze the data, and reconfigure the electrode head in the same application.

Ultimately, EIM will be used for taking a variety of measurements, including measurements on dynamically changing muscle. To make such measurements possible, the EIM system will have to be even faster at taking measurements. Preliminary work was done to determine the correlation between the minimum length of a measurement and the minimum frequency separation, since multi-frequency measurements are especially useful. Also, preliminary data was gathered which showed the potential for taking measurements at multiple orientations with respect to the muscle grain simultaneously.

Further clinical testing of the newest prototype system must be completed to ensure the reliability of EIM and the device. After this hurdle is overcome, EIM will be become an indispensable tool for neurologists and other health care professionals for quickly and consistently monitoring the evolving muscle health of their patients. This improvement in testing methods for devastating neuromuscular diseases will hopefully lead, in turn, to an overall improvement in these patients' health and happiness.

Appendix A

Schematics

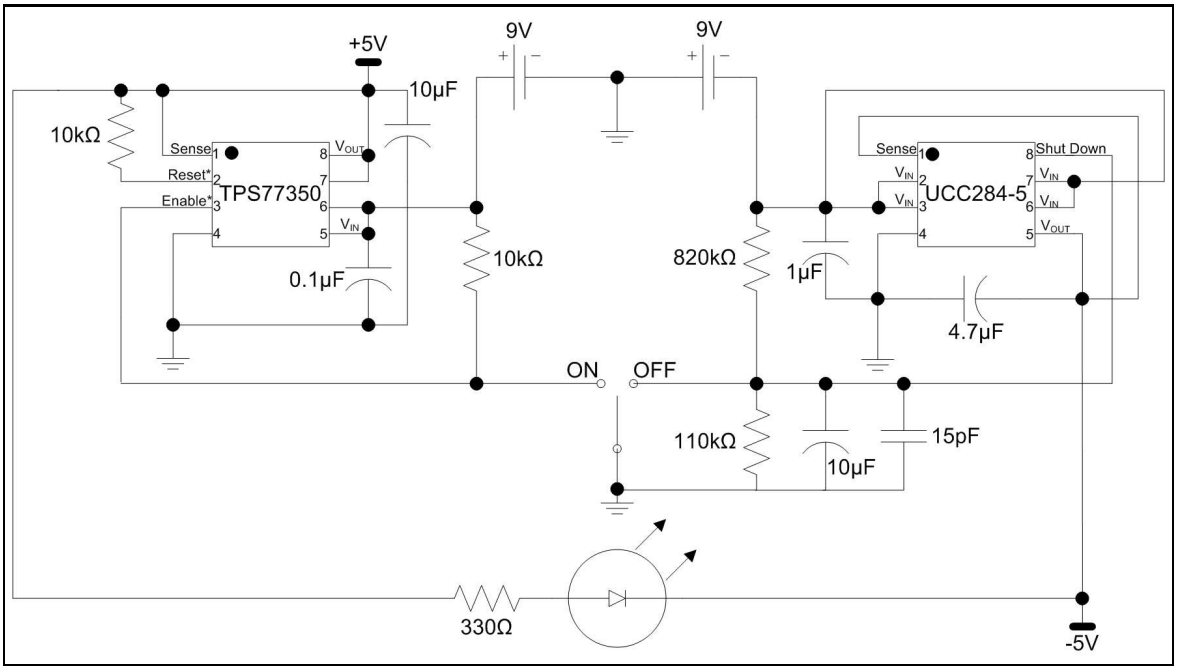

Figure A.1: Control Board Power Supply Schematic.

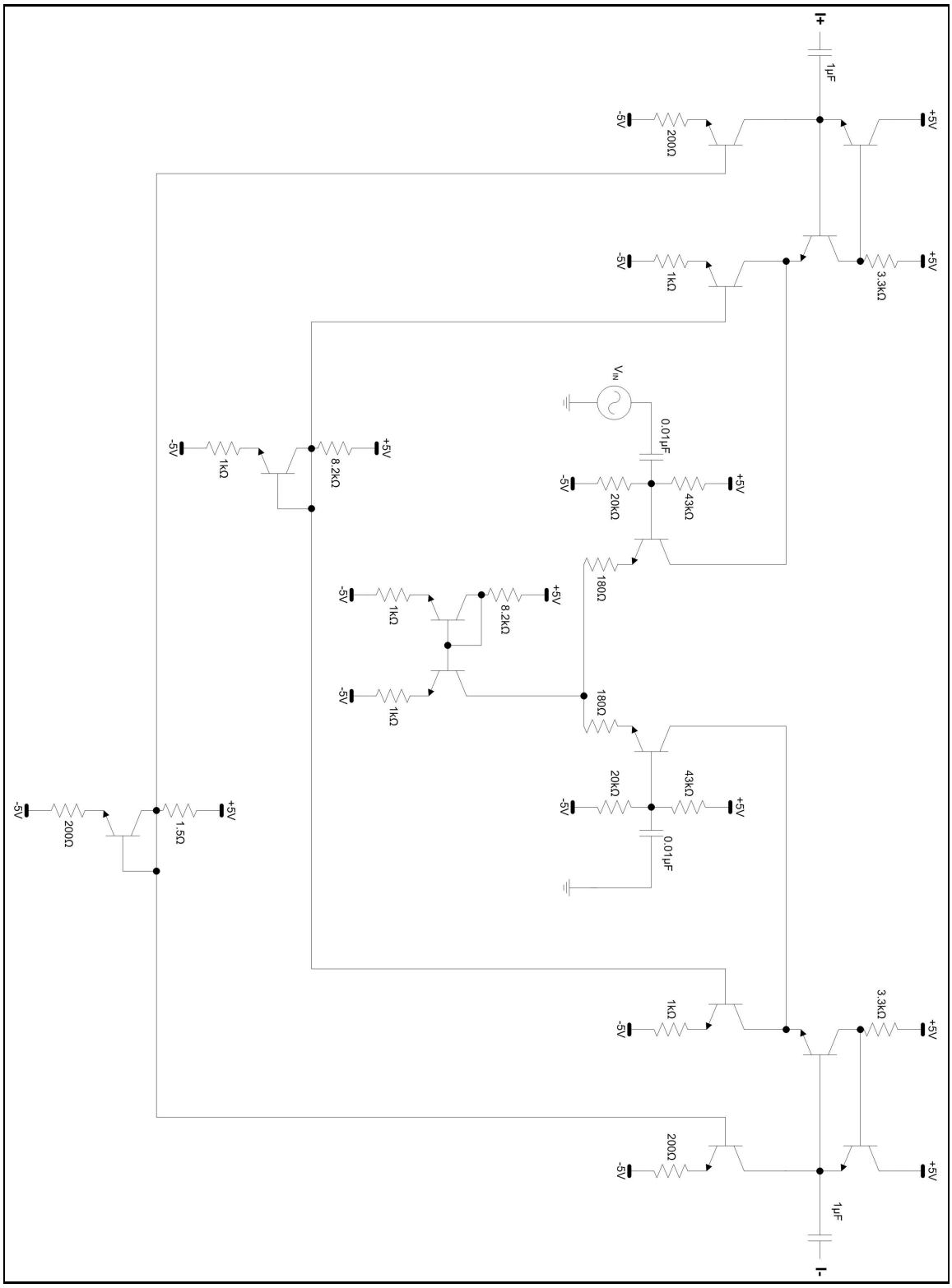

Figure A.2: Control Board Voltage Driver Schematic.

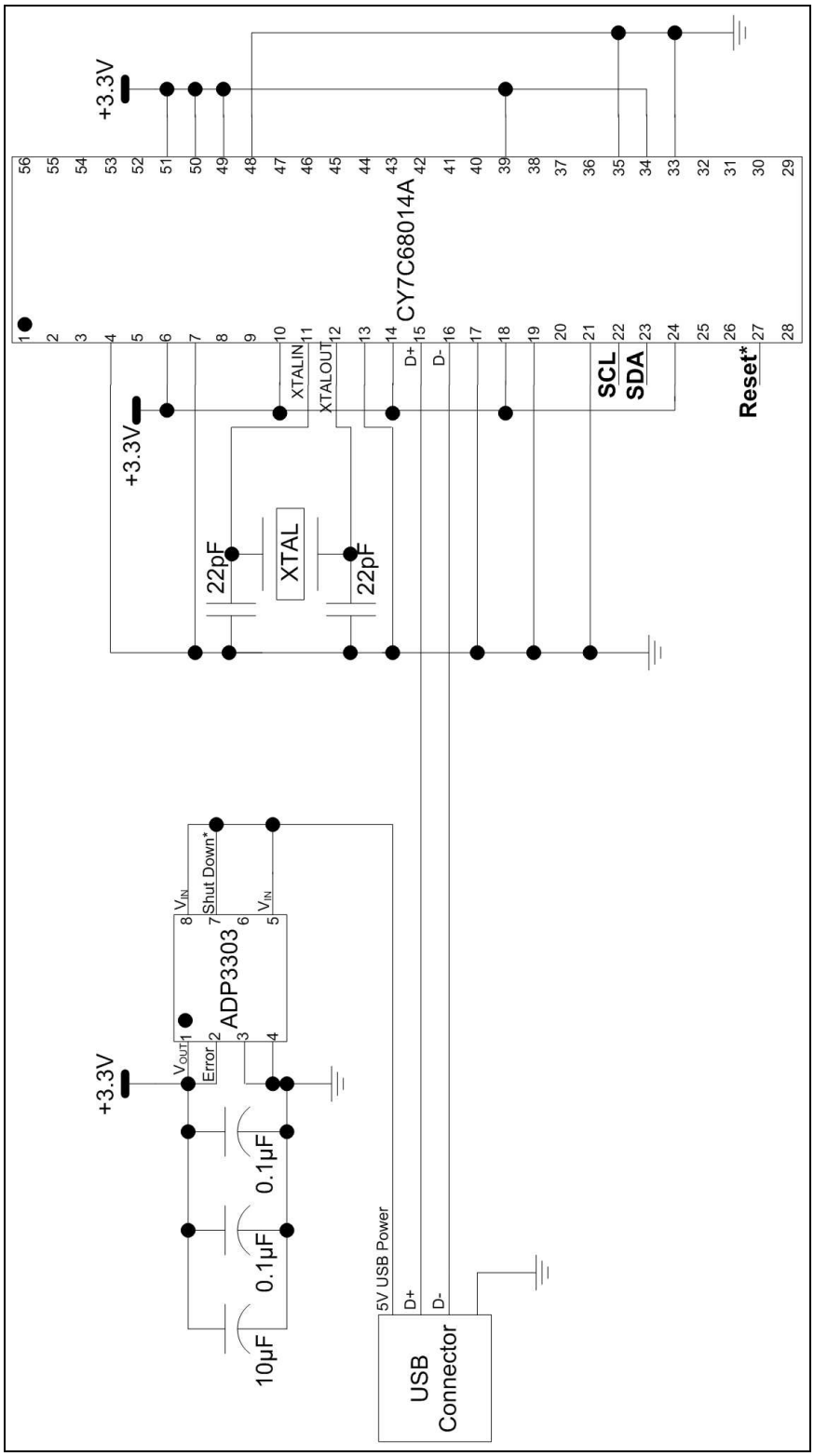

Figure A.3: Control Board Digital Control Schematic.

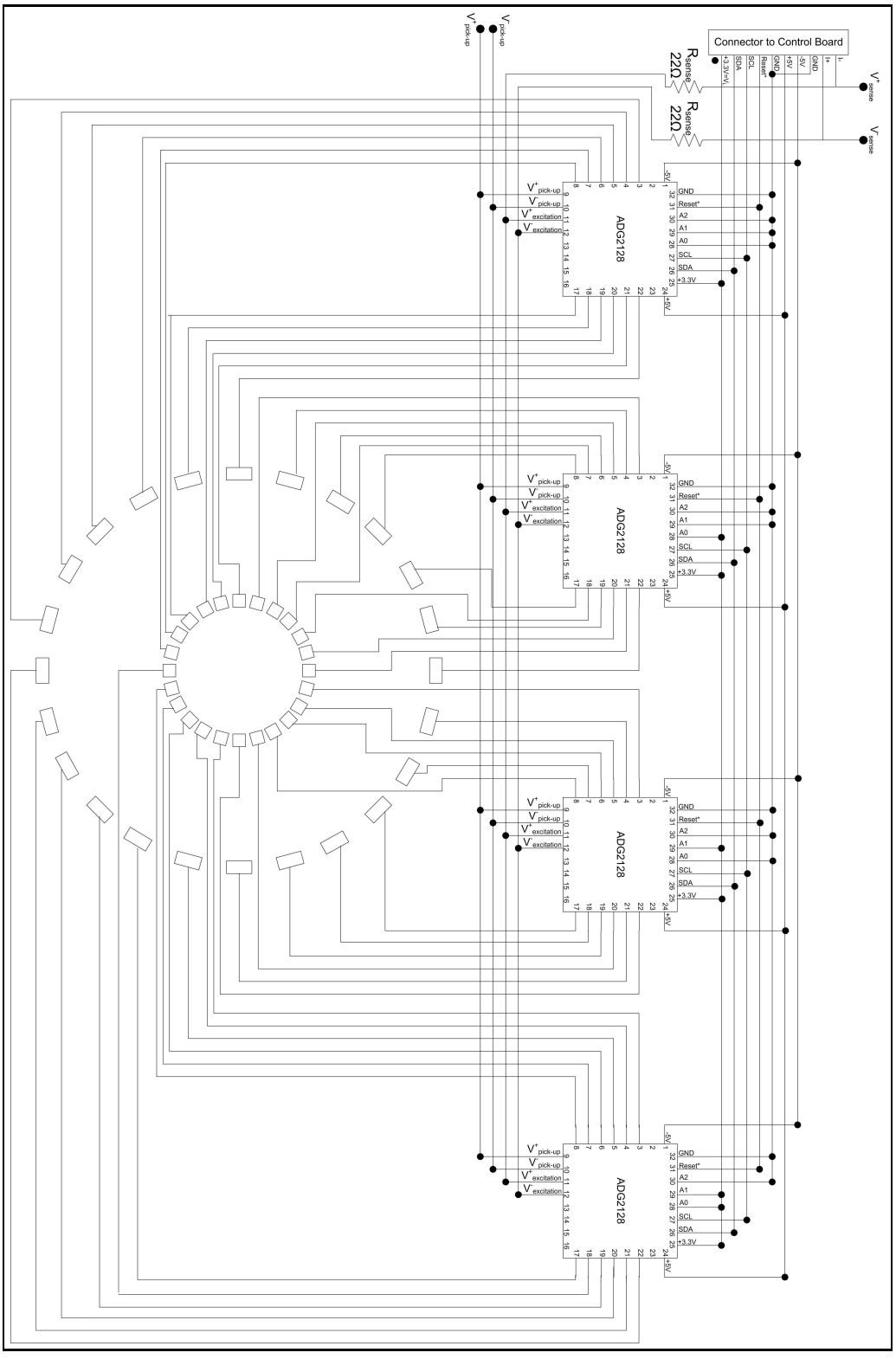

Figure A.4: Electrode Head Schematic.

Appendix B

XML File Example

Example XML file to setup the hand-held probe. This file causes the software to recognize 8 cells, and arrange them into one group of electrodes.

```
<cells>
   <cell>
      <id>0</id>
      <location>
         <x>3548</x>
         <y>1774</y>
      </location>
   </cell>
   <cell>
      <id>1</id>
      <location>
         <x>2750</x>
         <y>1774</y>
      </location>
   </cell>
   <cell>
      <id>3</id>
      <location>
         <x>3488</x>
         <y>2233</y>
      </location>
   </cell>
   <cell>
      <id>10</id>
      <location>
```

```
            <x>3488</x>
            <y>1315</y>
         </location>
      </cell>
      <cell>
         <id>24</id>
         <location>
            <x>0</x>
            <y>1774</y>
         </location>
      </cell>
      <cell>
         <id>25</id>
         <location>
            <x>798</x>
            <y>1774</y>
         </location>
      </cell>
      <cell>
         <id>27</id>
         <location>
            <x>60</x>
            <y>1315</y>
         </location>
      </cell>
      <cell>
         <id>31</id>
         <location>
            <x>238</x>
            <y>2661</y>
         </location>
      </cell>
      <cell>
         <id>34</id>
         <location>
            <x>60</x>
            <y>2233</y>
         </location>
      </cell>
   </cells>
   <electrodeHead>
      <electrode>
         <name>inner_000</name>
```

```
      <cellId>1</cellId>
   </electrode>
   <electrode>
      <name>outer_000</name>
      <cellId>3</cellId>
      <cellId>0</cellId>
      <cellId>10</cellId>
   </electrode>
   <electrode>
      <name>inner_180</name>
      <cellId>25</cellId>
   </electrode>
   <electrode>
      <name>outer_180</name>
      <cellId>27</cellId>
      <cellId>24</cellId>
      <cellId>34</cellId>
   </electrode>
   <group>
   <name>inner_000</name>
   <electrode>
         <name>inner_000</name>
         <output>0</output>
      </electrode>
      <electrode>
         <name>inner_180</name>
         <output>1</output>
      </electrode>
      <electrode>
         <name>outer_000</name>
         <output>2</output>
      </electrode>
      <electrode>
         <name>outer_180</name>
         <output>3</output>
      </electrode>
   </group>
</electrodeHead>
```

Appendix C

Fast Fourier Transform Algorithm

From Sedgewick and Kayne's *Introduction to Programming in Java: An Interdisciplinary Approach* [32].

```
// compute the FFT of x[], assuming its length is a power of 2
public static Complex[] fft(Complex[] x) {
   int N = x.length;

   // base case
   if (N == 1) return new Complex[] { x[0] };

   // radix 2 Cooley-Tukey FFT
   if (N % 2 != 0) { throw new RuntimeException("N is not a power of 2"); }

   // fft of even terms
   Complex[] even = new Complex[N/2];
   for (int k = 0; k < N/2; k++) {
      even[k] = x[2*k];
   }
   Complex[] q = fft(even);

   // fft of odd terms
   Complex[] odd = even; // reuse the array
   for (int k = 0; k < N/2; k++) {
      odd[k] = x[2*k + 1];
   }
   Complex[] r = fft(odd);
```

```
   // combine
   Complex[] y = new Complex[N];
   for (int k = 0; k < N/2; k++) {
      double kth = -2 * k * Math.PI / N;
      Complex wk = new Complex(Math.cos(kth), Math.sin(kth));
      y[k] = q[k].plus(wk.times(r[k]));
      y[k + N/2] = q[k].minus(wk.times(r[k]));
   }
   return y;
}
```

Bibliography

[1] R. Aaron, V. Amoss, K. Coomler, C. A. Shiffman, J. Therrien. "Resistivity and phase in localized BIA." *Physics in Biology and Medicine*, 44(10):2409-29, Oct 1999.

[2] R. Aaron, K. Bradonjic, G. Esper, K. Lee, S. Rutkove, C. Shiffman. "Effects of Age on Muscle as Measured by Electrical Impedance Myography." *Physiological Measurement*, 27(10):953-9, Oct 2006.

[3] R. Aaron, A. B. Chin, M. E. Cudkowicz, E. M. Raynor, S. B. Rutkove, J. M. Shefner, C. A. Shiffman, D. A. Schoenfeld. "Electrical Impedance Myography to Assess Outcome in Amyotrophic Lateral Sclerosis Clinical Trials." *Clinical Neurophysiology*, 118(11):2413-2418.

[4] R. Aaron, G. Esper, K. S. Lee, S. B. Rutkove, and C. A. Shiffman. "Assessing Neuromuscular Disease with Multifrequency Electrical Impedance Myography." *Muscle & Nerve*, 34(5):595-602, Nov 2006.

[5] R. Aaron, G. J. Esper, K. S. Lee, S. B. Rutkove, C. A. Shiffman. "Electrical Impedance Myography in the Detection of Radiculopathy." *Muscle & Nerve*, 32:335-341, 2005.

[6] R. Aaron, M. Huangy, and C. A. Shiffman. "Anisotropy of Human Muscle Via Non-invasive Impedance Measurements." *Physics in Medicine and Biology*, 42(7):1245-62, Jul 1997.

[7] R. Aaron, K. S. Lee, S. B. Rutkove, C. A. Shiffman. "Test-retest Reproducibility of 50kHz Linear-Electrical Impedance Myography." *Clinical Neurophysiology*, 25 Apr 2006.

[8] R. Aaron, S. B. Rutkove, C. A. Shiffman. "Electrical Impedance of Muscle During Isometric Contraction." *Physiological Measurement*, 24(1):213-34, Feb 2003.

[9] R. Aaron, S. B. Rutkove, and C. A. Shiffman. "Localized Bioimpedance Analysis in the Evaluation of Neuromuscular Disease." *Muscle & Nerve*, 25:390-7, Mar 2002.

[10] R. Aaron and C. A. Shiffman. "Angular Dependence of Resistance in Non-invasive Electrical Measurements of Human Muscle: the Tensor Model." *Physics in Medicine and Biology*, 43(5):1317-23, May 1998.

[11] R. Aaron and C. A. Shifman. "Using Localized Impedance Measurements to Study Muscle Changes in Injury and Disease." *Annals of the New York Academy of Sciences*, 904:171-180, May 2000.

[12] A. Al-Mudallal, Z. Argov, H. J. Kaminski, R. L. Ruff. "Toxic and Iatrogenic Myopathies and Neuromuscular Transmission Disorders." In: R. C. Griggs, D. Hilton-Jones, G. Karpati eds. *Disorders of Voluntary Muscle, 7th Edition.* Cambridge: Cambridge University Press, 2001:676-688.

[13] Analog Devices, One Technology Way, P.O. Box 9106, Norwood, MA 02062-9106, U.S.A. *ADG2128 Datasheet: I^2C CMOS 8×12 Unbuffered Analog Switch Array With Dual/Single Supplies*, May 2006.

[14] M. T. Andary, C. K. Jablecki, Y. T. So, D. E. Wilkins, F. H. Williams. "Literature Review of the Usefulness of Nerve Conduction Studies and Electromyography for the Evaluation of Patients with Carpal Tunnel Syndrome." *Muscle & Nerve*, 16:1392-1414, 1993.

[15] E. A. Beenakker, J. M. Fock, N. M. Maurits, J. H. van der Hoeven, D. E. van Schaik, et al. "Muscle Ultrasound in Children: Normal Values and Application to Neuromuscular Disorders." *Ultrasound in Medicine and Biology*, 30:1017-1027, 2004.

[16] H. J. Bittermann, H. Kele, C. D. Reimers, R. Verheggen. "The Potential Value of Ultrasonography in the Evaluation of Carpal Tunnel Syndrome." *Neurology*, 61:389-391, 2003.

[17] J. R. Buck, A. V. Oppenheim, R. W. Schafer. *Discrete-Time Signal Processing.* Prentice-Hall, 1999.

[18] A. B. Chin, J. L. Dawson, S. A. Ruehr, S. B. Rutkove, M. Scharfstein, A. W. Tarulli. "Saline-saturated Balsa Wood as a Testing Medium for Rotational Electrical Impedance Myography."

[19] A. B. Chin, K. S. Lee, S. B. Rutkove, A. W. Tarulli. "Impact of Skin-Subcutaneous Fat Layer Thickness on Electrical Impedance Myography Measurements: An Initial Assessment." *Clinical Neurophysiology*, 118(11):2393-7, Nov 2007.

[20] A. B. Chin, R. A. Partida, S. B. Rutkove, A. W. Tarulli. "Electrical Impedance in Bovine Skeletal Muscle as a Model for the Study of Neuromuscular Disease." *Physiological Measurement*, 27(12):1269-79, Dec 2006.

[21] W. C. Chumlea and S. S. Guo. "Bioelectrical Impedance and Body Composition: Present Status and Future Directions." *Nutrition Reviews.* 52(4):123-131, Apr 1994.

[22] Cypress Semiconductor Corporation, 198 Champion Court, San Jose, CA 95134-1709, U.S.A. *CY7C68013A EZ-USB FX2LP USB Microcontroller High-Speed USB Peripheral Controller*, Jan 2006.

[23] H. Evans, A. LeBlonc, R. Rowe, I. Shackelford, V. Schneider, S. West. "Muscle Atrophy During Long Duration Bed Rest." *International Journal of Sports Medicine*, 18 (Suppl. 4):S283-5, Oct 1997.

[24] J. L. Fleckenstein, W. Muller-Felber, D. E. Pongratz, C. D. Reimers, T. N. Witt. "Muscular Ultrasound in Idiopathic Inflammatory Myopathies of Adults." *Journal of the Neurological Sciences*, 116:82-92, 1993.

[25] J. L. Fleckenstein, C. D. Reimers, H. Schedel, et al. "Magnetic Resonance Imaging of Skeletal Muscles in Idiopathic Inflammatory Myopathies of Adults." *Journal of Neurology*, 241:306-14, 1994.

[26] A. Green, J. Jeppesen, J. Rahbek, B. F. Steffensen. "The Duchenne Muscular Dystrophy Population in Denmark, 1977-2001: Prevalence, Incidence and Survival in Relation to the Introduction of Ventilator Use." *Neuromuscular Disorders*, 13:804-12, 2003.

[27] M. G. Hochman and J. L. Zilberfarb. "Nerves in a Pinch: Imaging of Nerve Compression Syndromes." *Radiologic Clinics of North America*, 42:221-45, 2004.

[28] R. W. Kendall and R. A. Werner. "Interrater Reliability of the Needle Examination in Lumbosacral Radiculopathy." *Muscle & Nerve*, 34(2): 238-241, 2006.

[29] K. D. Mathews. "Muscular Dystrophy Overview: Genetics and Diagnosis." *Neurologic Clinics*, 21:795-816, 2003.

[30] K. Roeleveld and D. F. Stegeman. "What Do We Learn from Motor Unit Action Potentials in Surface Electromyography?" *Muscle & Nerve*, Suppl. 11:S92-7, 2002.

[31] M. Scharfstein. "A Reconfigurable Electrode Array for Use in Rotational Electrical Impedance Myography." Masters thesis, Massachusetts Institute of Technology. 72p, 2007.

[32] R. Sedgewick and K. Wayne. *Introduction to Programming in Java: An Interdisciplinary Approach*. Addison Wesley, 27 Jul 2007.

[33] Texas Instruments, P.O. Box 655303, Dallas, TX 75265, U.S.A. *TPS77350 250mA LDO Regulator with 8-PIN MSOP Packaging*, Jul 2001.

[34] Texas Instruments, P.O. Box 655303, Dallas, TX 75265, U.S.A. *UCC284-5 Low-Dropout 0.5A Negative Linear Regulator*, Feb 2002.

[35] TiePie Engineering, P.O. Box 290, 8600 Ag Sneek, The Netherlands. *MultiChannel Software User Manual*, 2007.

[36] TiePie Engineering, P.O. Box 290, 8600 Ag Sneek, The Netherlands. *Programmer's Manual: TiePie DLLs*, 2007.

[37] P. Wright. *Beginning Visual Basic 2005 Express Edition: From Novice to Professional* Berkeley, CA: Apress, 2006.